Bio-Synthesis and Characterization of Silver Nanoparticle and Silver-Bentonite Nanocomposite Using *Hagenia abyssinica* Leaf Aqueous Extract and Assessment of its Anti-Bacterial Activity.

Heledana Aderajew Hailu

A Thesis Submitted to

The Department of Applied Chemistry

School of Applied Natural Science

Presented in Partial Fulfillment of the Requirement for the Master of Science Degree in Applied Chemistry (Inorganic Chemistry)

Office of Graduate Studies

Adama Science and Technology University

March, 2022

Adama, Ethiopia.

Bio-Synthesis and Characterization of Silver Nanoparticle and Silver-Bentonite Nanocomposite Using *Hagenia abyssinica* Leaf Aqueous Extract and Assessment of its Anti-Bacterial Activity

Heledana Aderajew Hailu

Advisor: Dr. Eneyew Amare

A Thesis Submitted to Department of Applied Chemistry
School of Applied Natural Science

Presented in Partial Fulfillment of the Requirement for the Degree of Master of Science in Chemistry (Inorganic Chemistry)

Office of Graduate Studies
Adama Science and Technology University

March, 2022

Adama, Ethiopia.

Approval Sheet

We, the advisors of the thesis entitled "**Bio-Synthesis and Characterization of Silver Nanoparticle and Silver-Bentonite Nanocomposite Using *Hagenia abyssinica* Leaf Aqueous Extract and Assessment of its Anti-Bacterial Activity**" and developed by Heledana Aderajew, hereby certify that the recommendation and suggestions made by the board of examiners are appropriately incorporated into the final version of the thesis.

Advisor	Signature	Date

We, the undersigned, members of the Board of Examiners of the thesis by Heledana Aderajew Hailu have read and evaluated the thesis entitled **"Bio-Synthesis and Characterization of Silver Nanoparticle and Silver-Bentonite Nanocomposite Using *Hagenia abyssinica* Leaf Aqueous Extract and Assessment of its Anti-Bacterial Activity"** and examined the candidate during open defense. This is, therefore, to certify that the thesis has been accepted in partial fulfillment of the requirement of the Degree of Masters in Inorganic Chemistry.

Chairperson	Signature	Date
Internal Examiner	Signature	Date
Dr. Endale Tsegaye		March 21, 2022
External Examiner	Signature	Date

Final approval and acceptance of the thesis is contingent upon submission of its final copy to the Office of Postgraduate Studies (OPGS) through the Department Graduate committee (DGC) and School Graduate Committee (SGC).

Department Head	Signature	Date
School Dean	Signature	Date

Office of Postgraduate Studies, Dean	Signature	Date

Declaration

I hereby declare that the Master Thesis entitled "**Bio-Synthesis and Characterization of Silver Nanoparticle and Silver-Bentonite Nanocomposite Using *Hagenia abyssinica* Leaf Aqueous Extract and Assessment of its Anti-Bacterial Activity**" is my original work. It has not been submitted for the award of any academic degree, diploma or certificate in any other university. All sources of materials that are used for this thesis have been duly acknowledged through citation.

Name: Heledana Aderajew Hailu

Signature:_____

Recommendation

I, the advisor of the thesis, hereby certify that, I have read the revised version of the thesis entitled "**Bio-Synthesis and Characterization of Silver Nanoparticle and Silver-Bentonite Nanocomposite Using *Hagenia abyssinica* Leaf Aqueous Extract and Assessment of its Anti-Bacterial Activity**". Prepared under my guidance by Heledana Aderajew submitted in partial fulfillment of the requirements for the degree of Master's of Science in inorganic chemistry. Therefore, I recommend the submission of revised version of the thesis to the department following the applicable procedures.

Name of major Advisor	Signature	Date

ACKNOWLEDGMENT

First and foremost, I am grateful to the Almighty of God for blessing invaluable gift of health, wellbeing, strength, protection and accurate insight into reality for his divine intervention during my research work. Although this thesis work ultimately represents my accomplishments, had it not been the will of God, nothing would have been possible for me.

I am very thank full and want to appreciate my advisor Dr. Eneyew Amare, for his advice, guidance, patience and facilitating my thesis work.

I would also like to extend my gratitude to Adama Science and Technology University for providing the necessary knowledge, assistance and facilities to conduct my research work.

Especial thank goes to my aunt Woyenshet Sirak for Offering her money and time. I want to thank my family who were big sources of inspirations throughout my academic career with their valuable moral support and advice. Thank you to my best sisters Bezawit and Yanet Aderajew for your support and scarification.

At last, I would also like to thank my friends Melaku Mekuria Haymanot Zegeye, Rachel Worku, Nigatu Bejigo, Yosef Dentamo, Ruth Sahelu and Tzebet for their help and appreciated friendship.

Table of Contents

LIST OF TABLES

LIST OF FIGURES

LIST OF ABBREVIATIONS

ADT	Agar Diffusion Technique
Ag-Bent	Silver-Bentonite
AgNPs	Silver Nanoparticles
AAS	Atomic Absorpition Spectroscopy
DMSO	Dimethylsulpoxide
E.Coli	*Escherichia Coli*
FTIR	Fourier transform infrared spectroscopy
FWHM	Full Width Half Maxima
H. abyssinica	*Hagenia abyssinica*
MHA	Muller-Hinton Agar
MMT	Montmorillonite
NCs	Nanocomposites
NPs	Nanoparticles
S.aureus	*Staphylococcus aureus*
SPR	Surface Plasmon Resonance
UV-Vis	UV-Visible Spectroscopy
XRD	X-ray Diffraction

ABSTRACT

In this study, rapid, simple approach was applied for synthesis of environmental friendly nano-material. Silver Nanoparticles (AgNPs) and Silver Nanoparticle Bentonite (Bent) Nanocomposite (Ag-Bent NCs) were prepared using H. abyssinica leaf extract as reducing and capping agent for antibacterial application. Various advanced techniques like: X-ray diffraction (XRD), Fourier-transform infrared (FTIR) spectroscopy Ultraviolet-visible (UV-Vis) spectrophotometer and Atomic absorption spectroscopy (AAS) were used to characterize bentonite, AgNPs and Ag-Bent NCs for the phase analysis, crystallites size, functional group and compositional analysis respectively. UV-Visible spectrophotometer revealed the absorbance peak in range of 410-423nm for AgNPs and 368nm of AgNPs and 488nm of Bentonite in Ag-Bent NCs. XRD analysis result indicated that the synthesized AgNPs and Ag-Bent NCs found to possess a FCC structure. The average crystallite size of the Ag NPs estimated from XRD diffraction pattern using Debye Scherrer's formula was found to be 21.76nm for the 1:4 ratio of $AgNO_3$ to leaf extract in volume that capped nanomaterial and has a smaller particle size than the others. XRD results for Ag-Bent show that Ag NPs and bentonite are well combined in synthesizing Ag-Bent NCs. The FTIR analysis shows the presence of hydroxyl, carbonyl, alkyl, amide, alcohol and nitro functional group in NPs and NCs. And also shows the weak interaction between silver nanoparticles with the surface of Bentonite due to the presence of van der Waals interactions. AgNP demonstrated high-antibacterial activity against Staphylococcus aureus (Gram positive) as evaluated by means of inhibition zone of 15nm and Ag-Bent is good for both gram positive and negative bacteria but best for gram negative (Escherichia coli) bacteria with inhibition zone of 20nm, compared to ciprofloxacin which was used as a positive control in Agar disk diffusion method.

Keywords: *Bentonite, Nanocomposite, Silver nanoparticles, H. abyssinica, Antibacterial activity.*

CHAPTER 1

INTRODUCTION

1.1. Background of the Study

Developments of inorganic antibacterial materials that inhabit bacterial growth have been of great interest in recent years due to the increasing of antibiotics resistance bacteria and their potential use in everyday products [1]. Antibacterial inorganic materials based on metallic ion with antibacterial properties, like Silver (Ag^{+}),Copper (Cu), Titanium(Ti), Zinc (Zn) and Gold (Au) which are loaded on to clay [2,3] zeolite [4,5] and other have been used as a carriers with good results due to their high ion exchange capacity, high surface area and sorptive capacity, negative surface charge, chemical inertness and low or null toxicity [6]. Metal and metal oxide nanoparticles have gained a lot of attention as antibacterial materials. Nanoparticles are fascinating because of their high reactivity due to the large surface area to volume ratio [7].

From metal nanoparticles, silver(Ag) metal is used in many cases for disinfection, as coatings as well as in ionic or nanoparticulate form [8]. It has been known for its antibacterial and therapeutic capabilities for ages. As a result, Ag-based compounds have become increasingly popular as antibacterial agents [9]. These agents included Ag nanoparticles [10], Ag nanocomposite [11] and Ag sulfadiazine [12]. On the other hand, there are also various innovative Ag based products which have been produced and studied recently such as sutures modified by Ag-loaded montmorillonite [13], Ag nanoparticle–ionic silsesquioxane [14], nano-Ag fluoride in treating dental decay in children [15] and incorporation of silver nanoparticles into acrylic bone cement [16]. Silver Nanoparticles (AgNPs) have attracted a lot of attention among noble metal nanoparticles because of their appealing physicochemical features. Various researchers have been reported in biological science, drug delivery, water treatment, and as an antibacterial compound against both Gram (+) and Gram (-) bacteria [17].

Considering that such nanomaterials can be hazardous and fatal, hybrid processes in combining nanoparticles with other environmentally friendly, inert and stable materials is underway to take advantage of their full properties in various applications. Furthermore, combining nanoparticles with other substrates/fillers would result in composites with

innovative and enhanced capabilities that the separate components could not achieve. The nanoparticle must be applied on substrates such as graphite, zeolite, carbon nanotubes, clays, or polymer materials in order to be used as an antibacterial agent [18].

In this regard, clay mineral-based antibacterial complexes have been developed by a variety of method involving between the clay minerals and antibacterial substances to increase the strength of the interactions between clay and NPs. Clay minerals are hydrated alumino-silicates that contain alkaline and alkaline earth metals in general. They are great fillers for metal composites and good metal ion supporters [19]. Clays such as montmorillonite, sepionite, bentonite, palygorskite, halloysite and zeolite are being considered as low-cost fillers and commonly used supporting substrates for nanoparticles [18].

Among the clay, bentonite is considered as the main source in bioactive fields. It consists of microcrystalline particles of montmorillonite (MMT) which belongs to 2:1 phyllosilicate clays which mean that it has one octahedral sheet of aluminum ions sandwiched between two tetrahedral sheets of silicon ions. The structural characteristics and multifarious application of bentonite are improved by replacing exchangeable inorganic cations (e.g. Na^{+},Ca^{2+},H^{+},K^{+}) on the interior and exterior surfaces with inorganic cations such as Ag nanoparticles [20]. Because of its low cost and availability as well as its stable mechanical and chemical property, bentonites are being used for ion exchange and adsorption applications [21], Because of this feature, they can be used for incorporation of various positively (cationic) charged inorganic compounds.

In this work, we present a simple method for the preparation of silver nanoparticles (AgNPs) and Silver –Bentonite nanocomposite (Ag-Bent NCs) using the leaf of *H. abyssinica* under different characterizations and antibacterial activity. The plant is chosen as a reducing agent for the synthesis of Ag nanoparticles. Bentonite was used as the protective colloid preventing the Ag NPs from aggregation. The antibacterial activities of the samples were investigated and compared with one another.

1.2. Statement of the Problem

In recent years, the continuous emergence of resistant or multi-resistant strain of microorganisms towards the drugs used clinically raises the need for the search of new antimicrobials substance and different antibacterial activities have been developed from

different materials. For centuries, people have used silver for its antibacterial qualities. Silver nano have better qualities than the bulk one.

Silver nanoparticles (AgNPs) are widely used in a growing number of applications due to their unique properties. However, with the accelerating introduction of AgNPs into commercial products, there is likelihood of their release into the environment, which gives rise to health and environmental concerns, as it is reported that the type of incorporation greatly affects the nanoparticle release.

In the last few years, clay mineral-based antibacterial complexes have been prepared using a variety of methods that strengthen the bond between clay minerals and antibacterial nanoparticles. According to researchers, clays has no adverse effect, is abundant, non-toxic and inexpensive, has a great adsorption properties, and is environmentally being. Silver nanoparticle loaded into bentonite which would improve the binding ability of silver with the clay and reduce the release of silver into environment, interact with soil and sediment to form inert aggregate and enhance the antibacterial activity of the silver nano-particle.

Therefore, in this research it is intended to synthesis, characterize silver nanoparticle and silver-bentonite nanocomposite using utilization of bioactive compounds present in *H. abyssinica* leaf aqueous extract for antibacterial application.

1.3. Objectives of the Study

1.3.1. General Objective

- The general objective of this study is to synthesis and characterizes Silver Nanoparticles and Silver- Bentonite Nanocomposite for antibacterial activities.

1.3.2. Specific Objectives

The Specific Objectives of this study are:-

- To synthesis AgNPs and Ag-Bent NCs using silver nitrate, activated bentonite and plant leaf extract and characterize using AAS, UV-vis, XRD and FT-IR.
- To assess the antibacterial activities of the synthesized AgNP and Ag-Bent NCs using agar diffusion method against gram negative (*Escherichia coli)* and gram positive (*Staphylococcus aureus).*

1.4. Significance of the Study

ıt is expected that this work will contribute to a better understanding of the synthesis of AgNPs and Ag-Bent NCs by using leaf extract. This work also provides the investigation results of anti-bacterial, Ag-Bent NCs, on the selected gram positive and gram negative strains. And also using locally available, environmentally friendly natural raw materials like clay and plant extracts may help to develop alternative and improved green antibacterial agents. Furthermore, report obtained here will provide documentary information that can be referred by other researchers interested to work.

CHAPTER 2

LITERATURE REVIEW

2.1. Clay Minerals

The term "Clay" refers to a naturally occurring material made up mostly of fine-grained minerals that is normally flexible and plastic when wet but hardens when dried or burnt. "Clay mineral" refers to phyllosilicate minerals, which are layer silicates that form at the earth's surface as a result of chemical weathering of other silicate minerals [22].

These materials are characterized by their extremely small size (a few micrometers at the most extreme) and their preferred development occurs under surface (alterites, soils, and residue) or subterranean (diagenesis and aqueous adjustments) environments [23]. Clays are lamellar aluminosilicates that have a variety of physicochemical properties, such as swelling, adsorption, ion exchange, and surface acidity [24]. They are important part of the phyllosilicates or sheet silicate family of minerals, which have layered structures composed of polymeric SiO_4 tetrahedral sheets linked to sheets of (Al, Mg, Fe)$(O,OH)_6$ octahedral [22].

Common clay minerals are Kaolinite (1:1phyllosilicates), Smectite (montmorillonite-MMT) (2:1phyllosilicates), Sepiolite (2:1invertedribbons), Illite(2(T):1(O)), Chlorite, and Vermiculite [25]. They are very different, even though each is composed of octahedral and tetrahedral sheets as their basic building blocks. However, the arrangement and composition of the octahedral and tetrahedral sheets account for most of the differences in their physical and chemical properties [23].

2.2. Bentonite Clay

From the smectite clay family, bentonite clay, which is an aluminum phyllosilicate clay material that mainly formed by aged volcanic ash known as “montmorillonite”, which their physical properties are established by this clay mineral. This substance resulted from the alteration of glassy material ejected from volcanoes or the alteration of silica-bearing rocks like granite and basalt during geological time. In addition to MMT it also contains a

variety of accessory minerals such as attapulgite, kaolin, mica, and illite, as well as minerals such as quartz, feldspar, calcite, and gypsum [21].

The chemical properties of bentonite can be altered by adding highly ionic, stable, and higher density species to the bentonite clay interlayer through an ion-exchange and sorption process. Thermal and chemical changes can improve the adsorption capability of bentonite. For enhancing the adsorption capacity of bentonite, a variety of surface modification techniques, including as heat and acid treatment, can be utilized [26].

2.2.1. Structure of Bentonite

This montmorillonite-based clay is characterized as a 2:1 phyllosilicate clay, with one octahedral sheet sandwiched between two silica tetrahedral sheets forming a unit crystal structure. Positive cations and water molecules make up the interlayer between units. Due to this crystalline arrangement, smectites are able to expand and contract the interlayer while maintaining two dimensional crystallographic integrity [7]. Because of its structure, it can be used as an antibacterial and antifungal carrier. The porous structure of bentonite is roughly divided into three categories: micropores, mesopores, and macropores, according to *Babaki, H.et al.* Micropores are smaller than 2nm, between 2nm and 50 nm are mesopores and larger than 50nm are macropores [27]

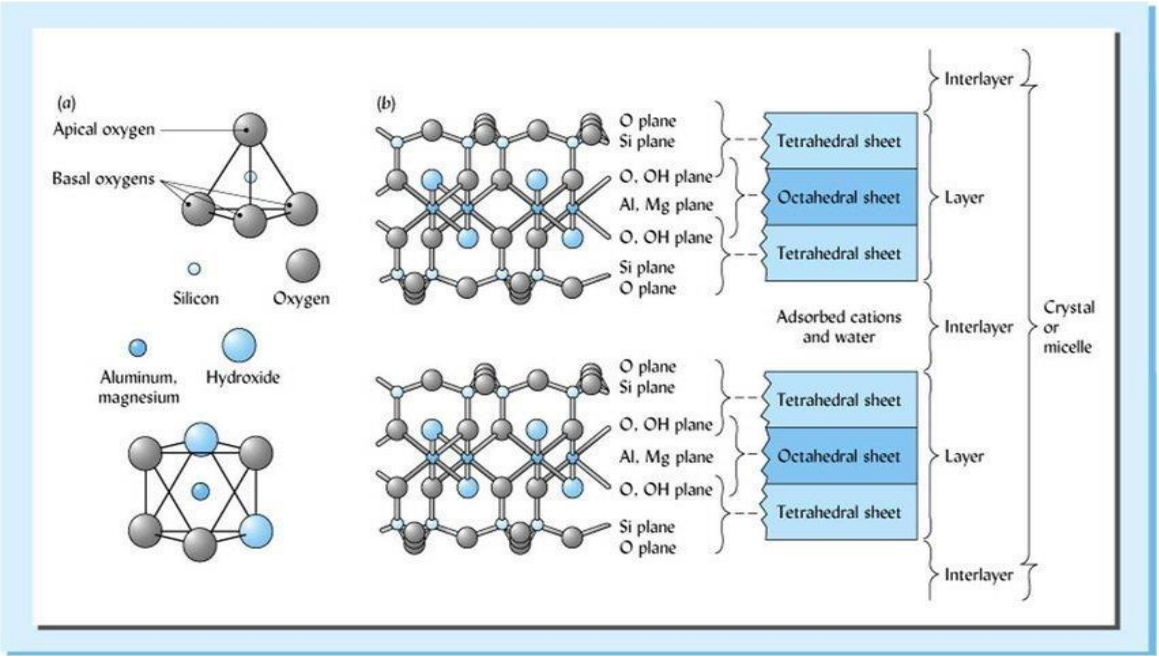

Figure 1: Diagram for the Structure of bentonite clay

As a result, they are classified as expandable 2:1 phyllosilicate clays with permanent charges that may interchange cations and anion. Both layers of these sheets contain oxygen atoms. These three –layer units are stacked (piled up) one on top of the other, with oxygen in surrounding layers next to each other. This results a weak bond, enabling water and other polar molecules to pass between layers and cause the mineral structure to expand (swelling). Silicon can be replaced by aluminum or iron in tetrahedral coordination [28]. Isomorphous substitution allows magnesium, iron, lithium, chromium, zinc, or nickel to be substituted for aluminum in the octahedral coordination. The different montmorillonite clay minerals are formed by differences in replacements within the lattice in terms of location and elemental content [29].The molecular formula for montmorillonite is usually expressed as:

$(1/2Ca, Na)(Al,Mg,Fe)_4(Si,Al)_8O_{20}(OH)_4 .xH_2O$, general chemical formula [30]

2.2.2. Types of Bentonite Clay

Bentonite clay can be classified in to K, Na, Ca, and Al bentonite depending on the dominant element constituent, but the main two types Sodium (Na) and Calcium (Ca) are recognized, and the uses of each depend on specific physical properties.

2.2.2.1. Sodium Bentonite

Sodium bentonite has a single water layer particles that contain Na^+ as the exchangeable ion. When wet, it swells and absorbs up to several times its dry mass in water. Swelling of bentonite is mostly induced by montmorillonite swelling [31]. This swelling is an important property of clay mineral, because of this it is the most useful that can absorbs large quantities of water and swelling to many times their original volume and gives rise to permanent suspension of gel like masses [32].They are mainly used as bonding clay for different applications.

2.2.2.2. Calcium Bentonite

Calcium bentonite is a useful adsorbent of ions in solution, as well as fats and oils. It has a double water layer with Ca^{2+} as the exchangeable ion. Calcium bentonites are non-swelling and break down to finely granular aggregate that is widely used as an absorbent clay sometimes called fuller's earth [32].

By using an ion exchange method, calcium bentonite may be transformed to sodium bentonite (also known as sodium activation or sodium beneficiation) to display several of sodium bentonite's properties. Using a soluble sodium salt, such as sodium carbonate, and by soda activation has high montmorillonite content. Some properties of sodium-beneficiated calcium bentonite (or sodium-activated bentonite) are high swell potential, small particle size, and high specific surface area than Ca-montmorillonite [33].

2.2.3. Properties of Bentonite Clay

The widespread use of bentonite can be attributed to its physical and chemical properties such as small particle size, high porosity, large surface area and high cation exchange capacity. It has excellent adsorption capacity and its adsorption ability is determined by the chemical nature and pore structure [34]. The physico-chemical properties such as adsorption capacity largely depend on the presence micro and mesopores; and, the effect of macropores is found to be insignificant [27]. The exceptional adsorption properties and cationic exchange capacity originated from the fundamental crystalline arrangement, which consists of two tetrahedral layers of silica connected by one octahedral layer of alumina. Each one is separated by an interlayer gap, which contains exchangeable cations (Na^{+}, Ca^{2+}, Mg^{2+}) to counteract the structural superficies' apparent negative charge caused by isomorphic replacements of less-charged cations in the octahedral sheet [35].

Bentonite clay is naturally highly absorbent and has supercharged electrical energy that produces a strong negative charge that aids in the removal of positively charged heavy metals and poisons from the body. It has antimicrobial properties. As a result, it can be used to treat and cure diseased skin diseases caused by microbial infections [36]. It is also has particular potential to eliminate inorganic and organic contaminant from the surroundings because of its mechanical stability, chemical inertness, abundance, distinctive structural properties and large surface areas [37].

And other properties like

- It is an odorless grey/cream color with an almost soft, very fine consistency. Unlike some other clays, it doesn’t stain and is easy to work with in beauty and natural remedy recipes.

- Healing clays like bentonite have a high concentration of minerals including silica, calcium, magnesium, sodium, iron, and potassium. It also absorbs and removes toxins, heavy metals, impurities, and chemicals.
- It is a common ingredient in detox and cleansing products. Common external uses include poultices, mud packs, detox baths, and skin care recipes.
- Bentonite clay is a unique clay due to its ability to produce an "electrical charge" when hydrated. Upon contact with fluid its electrical components change, carrying a strong negative charge which bonds to the positive charge in many toxins. When it comes in contact with a toxin, chemical, or heavy metal, the clay will absorb the toxin and release its minerals for the body to use. Bentonite also helps get oxygen to cells as it pulls excess hydrogen and allows the cells to replace it with oxygen instead.

2.2.4. Antibacterial Activity of Bentonite Clay

Bentonite is a widely distributed, low-cost mineral that possesses high ion adsorption, porosity, and microbial adhesion, as well as being environmentally friendly [38]. It is also considered as the main source in bioactive fields and it has been used in ancient and modern medicines because of their special layer structures, specific surface areas, cation exchange capacity, and a wide range of multifarious and potential biomedical applications. Its microcrystalline particles of montmorillonite which may interact strongly with certain antimicrobials, affecting their bioavailability [20]. Potentially, this interaction can be highly advantageous in the design of modified-release systems for the controlled administration of antibacterial substances, which nowadays is one of the most interesting fields for pharmaceutical and veterinary applications [39]. As the montmorillonites layer structure gives the antimicrobial and antifungal carrier, it has the property of antibacterial and it can adhere to pathogens and excrete them, reinforce intestinal mucosal barrier and help regeneration of epithelium [40]. Pharmacology studies have revealed that montmorillonite (MMT) adsorbed bacteria such as *E. coli, S. aureus* and immobilize cell toxins [41].

2.3. Silver Metal and Silver Nanoparticles

2.3.1. Silver for Antibacterial Activity

Silver (Ag) is the metal of abundance, among the gracious metals for future applications in the areas of living organisms and biological systems. As it is a noble metal, silver is not attacked by water or acids. However, silver metal continuously releases small amounts of ions, which act antibacterially at the metal surface [8]. It has a long history of use in medicine as an antimicrobial agent. Silver ions have been found to have antibacterial effects on some microbes. Several studies have demonstrated that silver ions are selectively toxic for prokaryotic microorganisms, with little effect on eukaryotic cell [42]. *I. Sondi and B. Salopek-Sondi* reported that silver ions and silver-based compounds are highly toxic to microorganisms showing strong biocidal effects on as many as 16 species of bacteria including *E. coli* [43].

Silver is generally used in the nitrate form to induce the antimicrobial effect but when silver nanoparticles are used, there is a huge increase in the surface area available for the microbes to be exposed. Hernández Sierra *et al* compared the anti-Streptococcus mutans activity of nano scale silver, gold, and zinc oxide and found that silver nanoparticles (AgNPs) worked best [44]. Antibacterial activity against *Aspergillus niger, Bacillus subtilis, S. aureus, E. coli, Proteus vulgaris* and other investigations also reported the better results [43].

Silver is a well-known antibacterial agent against more than 650 microorganisms from various classes such as gram-positive and gram-negative, fungi or viruses. The material has recently found use in the form of silver nanoparticle. Out of the metals with antimicrobial properties, it was found that silver has the most effective antibacterial action and is the least toxic to animal cell [45].

2.4. Nanotechnology

In this era, nanotechnology is one of the most interesting area which is used to describe the creation and utilization of materials with structural features between those of atoms and bulk materials with at least one dimension in the nano range [46]. Nanotechnology refers to any technology that is implemented at the nanoscale and has applications in the real world. It has been defined as research and development at the atomic, molecular and

macromolecular scale. It is also defined as the control or restructuring of matter at the atomic and molecular levels in the size range of about 1 to 100 nm [47]. Nanoscale materials find use in a variety of different areas, such as electronic, magnetic and optoelectronic, biomedical, pharmaceutical, cosmetic, energy, environmental, catalytic, and materials applications [48]. The properties of matter at the nanoscale are different from those at a larger scale. The unique physical and chemical properties of nanomaterials can be exploited for commercial applications and for novel performance that benefits society [49]. Because of the potential of this technology, there has been a worldwide increase in investment in nanotechnology research and development.

2.5. Nanoparticles

Nanoparticles are considered to be the building blocks for nanotechnology and are referred to particles with at least one dimension <100 nm [48]. Nanoparticles have a nanoscale dimension, and they are very small sized particles with enhanced catalytic reactivity, thermal conductivity, non-linear optical performance and chemical steadiness owing to its large surface area to volume ratio. Surface area to volume ratio in nanoparticles have a significant effect on the nanoparticle's properties. The application of nanoparticles have been used in different industry, health, food, space, chemical and cosmetics industry depending on the nano scale dimension of the nanomaterial [50]. Nanoparticles are of great scientific interest as they are a bridge between bulk substances and their molecular or atomic structure. A bulk substance has constant physical and chemical properties irrespective of its size; nevertheless, at the nanoscale these properties depend more or less on particle size [51]. The bulk particles have different properties from those of nanoparticles that have the same chemical substance. Nanoparticles basically change their properties of substance when their size is reduced to the nanometer range. When a bulk material is reduced into small size particles with one or more dimension (length, width, or thickness) in the nanometer range or even smaller, the individual particles show unexpected properties different from those of the bulk materials [52] .

2.5.1. Surface Area and Size

It has been found that properties vary with particle size. Particle size and surface area play a major role in interaction of materials with biological system. Seemingly, decreasing the

size of the materials leads to an exponential increase in surface area to volume ratio, thereby making the nanomaterial surface more reactive [51].

2.5.2. Approaches for the Synthesis of Nanoparticles

There are two general approaches for synthesis of nanomaterials; top-down and bottom-up approach [53]. These approaches further divide into various subclasses based on the operation, reaction condition and adopted protocols [54]. Fig. 2 shows bottom up and top down approaches subclass:

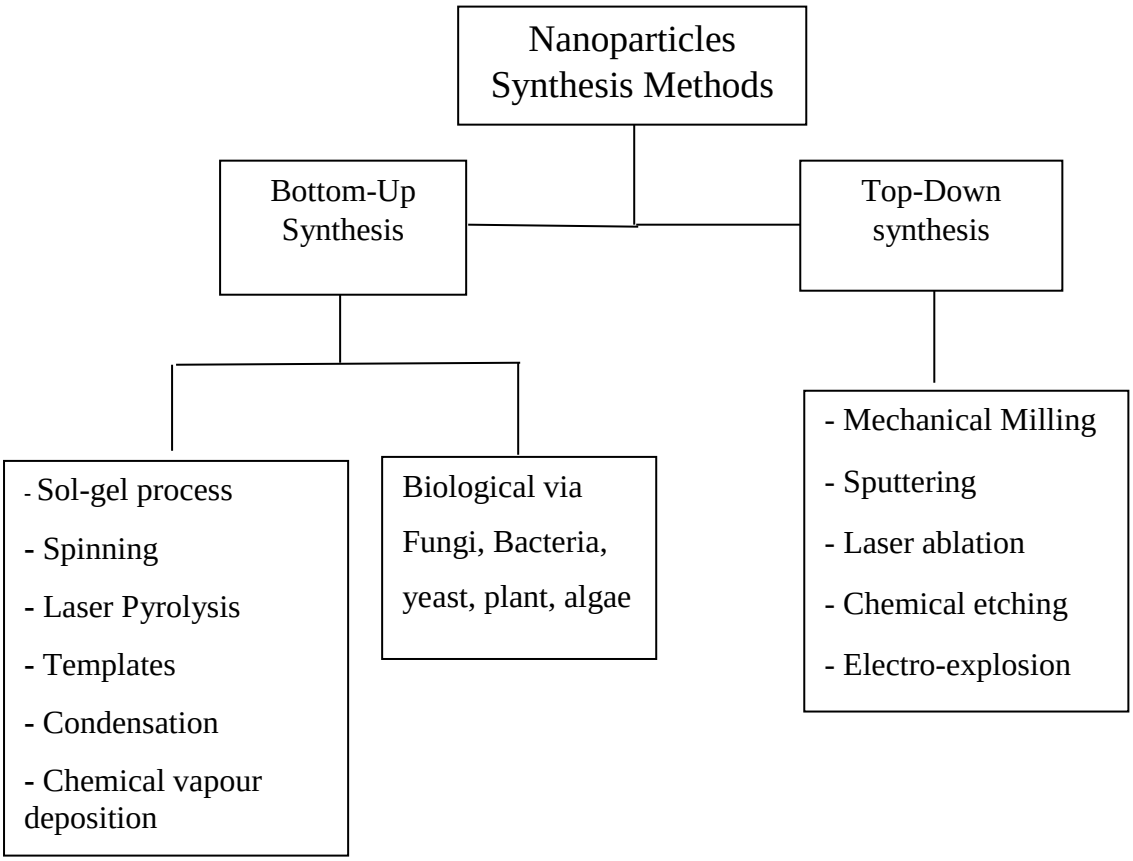

Figure 2: Approaches for the synthesis of Nanoparticles [55]

From Figure 2 top down approach is destructive approach starting from larger molecule, which decomposed into smaller units and then these units are converted into suitable NPs. Examples of this method are grinding/milling, physical vapor deposition (PVD) and other decomposition techniques [54]. Bottom up approach is employed in reverse as NPs are formed from relatively simpler substances; therefore this approach is also called building up approach. Examples of this case are sedimentation and reduction techniques. It includes sol gel, green synthesis, spinning, and biochemical synthesis [54]. In another way, there

are three basic methods for the synthesis of nanoparticles named physical, chemical and biological methods.

Physical and chemical methods are widely used for the synthesis of nanoparticles, unfortunately, these methods have some drawbacks such as their use of high energy or hazardous chemicals, great expense and production of large amounts of toxic byproducts that create environmental contamination. To overcome these limitations of physical and chemical methods, ecofriendly, facile, low cost and nontoxic methodologies are essential for metal nanoparticle synthesis by avoiding the use of toxic and expensive chemicals and solvents. Recently, biological synthesis of metal nanoparticles has been highlighted, which is safe, ecofriendly, facile, nontoxic and economical [56].

2.6. Green synthesis of Nanoparticles

Biosynthesis of nanoparticles is a method of synthesizing nanoparticles with biomedical uses utilizing microbes and plants. This method is eco-friendly, cost-effective, biocompatible, safe, and environmentally beneficial. Plants, bacteria, fungi, algae, and other organisms are all used in green synthesis [57]. NPs synthesized from biomimetic approach show more catalytic activity and limit the use of expensive and toxic chemicals.

Bio-reduction involves reducing metal ions or metal oxides to 0 valence metal NPs with the help of phytochemicals like polysaccharides, polyphenolic compounds, vitamins, amino acids, alkaloids, terpenoids secreted from the plant [53-54]. So, green synthesized nanoparticles have a wide range of applications in the food, pharmaceutical, and cosmetic industries, and have thus become a prominent study topic. This calls for an alternative method known as biogenic/biosynthesis that is more biocompatible, facile, and non-toxic. Biosynthesis procedures produce nanoparticles that are more stable using various plant leaves, roots, fruits, and seeds extract that are rich in flavonoid, phenol, tannin, amino acid, and alkaloid phytochemicals as a reducing agent for the synthesis

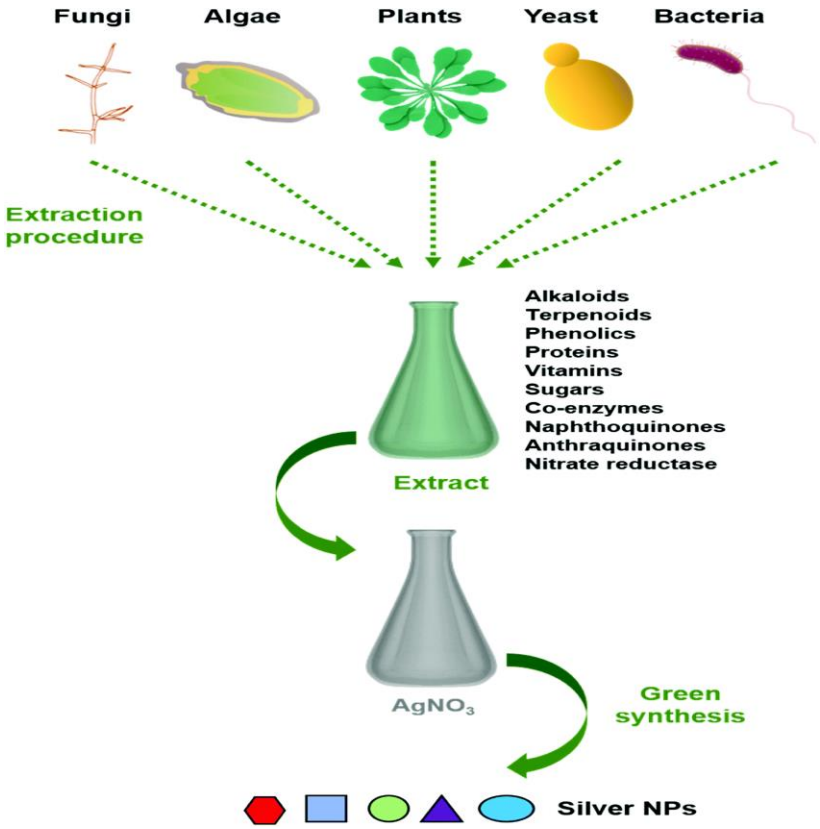

Figure 3: Schematic illustration of the procedure for green synthesis of silver nanoparticles [59].

Plant parts like leaf, stem, root, fruit, and seed have been used for Ag NPs synthesis because of the exclusive phytochemicals that they produce. Natural extracts of plant parts are a very environmentally friendly and inexpensive procedure that does not require the use of any intermediate base groups. It takes a less of the time, requires no expensive equipment or precursors, and produces a highly pure and quantity-enriched product devoid of impurities [58].

Plants are the most preferred source of environmentally friendly Stabilizer for NPs synthesis because they allow for large-scale production and the creation of stable nanoparticles of various shapes and sizes [59]. Among them, plant-based materials are the best candidates, because it is believed that polyphenols present in their composition are the active key to the synthesis [60]. There have been several studies on the synthesis of AgNPs using various plants such as *manilkarazapota(L) seed* [61], *Rosmarinus leaf* [62], *Fritillaria flower* [63], *Allium rotundum l, Falcaria vulgaris Bernh, and Ferulago angulate Boiss* [64], *Artemisia Absinthium* [65], *Latex of Jatropha curcas* [66],*Capsicum anannuum* [67], *Mulberry leaves* [68], *Cinnamomum camphora* [69]. Use of plants in

synthesis of nanoparticles is quite novel leading to truly green chemistry which provide advancement over chemical and physical method [70].

2.6.1. Green synthesis of Silver nanoparticle

Silver nanoparticles (AgNPs) are among the noble metal nanoparticles that have a wide area of interest since they have too many applications in difference field. Because of these applications, many methods for synthesis of AgNPs have been developed [71], including biological, chemical, photochemical and electrochemical processes. *Krithiga, N et al* reported the chemical reduction using hazardous reducing agents, such as sodium borohydride, formaldehyde and ammonia is typically employed for AgNPs preparation, limiting the use of AgNPs for biological or medical applications [70]. AgNPs are accounted to acquire effective antiplatelet, antifungal, antiviral, antimicrobial agent and anti-inflammatory against different pathogens [72]. Some antimicrobial agents are extremely irritant and toxic and there is much interest in finding ways to formulate new types of safe and cost-effective biocidal materials [43].

The desire to develop an eco-friendly approach for the synthesis of nanoparticles has arisen as a result of growing awareness of green chemistry and other biological processes. This approach has several advantages, including simplicity, cost-effectiveness, compatibility for biomedical and pharmaceutical applications, as well as large-scale commercial production [73].

2.6.2. *Hagenia abyssinica* leaf for Silver nanoparticles synthesis

Hagenia abyssinica is the sole species of the genus *Hagenia* and belongs to a monotypic genus in the family *Rosaceae*, also it is most intimately interrelated to the monospecific genus Leucosidea [74]. *Rosaceae* is a large family containing more than 100 genera and 2,000 species of herbs, shrubs, and trees [75]. *Hagenia abyssinica* is a slender tree up to 20 m tall, with a short trunk and thick branches. The bark, flower, leaf, and root parts of *H. abyssinica* have been used for both medical and nonmedical purposes [76]. This dioecious tree species is known by its common name ‘kosso’ in Ethiopia. Currently, it is however sparsely distributed in mountainous areas in Central, South-western and South-eastern parts of Ethiopia. The species is also found in different parts of Africa such as Kenya, Tanzania, Burundi, Sudan, Democratic Republic of Congo, Malawi, Uganda and Rwanda

[77]. Historically, *H. abyssinica* has been one of the most famous plants of Africa since it was used by Merck of Germany already in 1870 for the production of kosins (phloroglucinols), a crystalline substance derived from the female flowers [78]. In Ethiopia female inflorescence dried flowers are traditionally used as an anthelmintic remedy, particularly it has been used for its potent anti-tapeworm activity and at one time was included in most European pharmacopoeias as an effective drug against intestinal worms [76]. The flowers contain Phloroglucinol derivatives similar to those of Dryopteris ferns [79]. *H. abyssinica* has been used as a remedy for intestinal parasites, especially against cestodes and it has served as an anthelmintic in ruminants and also against tapeworms in humans [80]. This strong medicine when taken in large quantities; it is sometimes taken as an abortifacient [81], in traditional medicine the extract is used as abortifacient which initiated investigations examining it as a potential contraceptive agent [74]. Also its roots are cooked with meat and the soup drunk for general illness and malaria, while bark hammered and added to cold water and the liquid drunk as a remedy for diarrhea and stomach-ache [82]. Besides being a source of medicine, *H. abyssinica* has been utilized for various other purposes such as construction, furniture, fuelwood, soil fertility management, as fertile soil formation, soil conservation, as well as rainwater conservation [76].

Figure 4: Image of *H. abyssinica* tree along with its flowers [83].

H. abyssinica plant provides a rich and rare combination of zeatin, and it is loaded in nourishment owing to the presence of essential phytochemicals, It is rich in phytochemicals particularly secondary metabolites such as tannins, terpenoids, flavonoids, Saponins, alkaloids, phlobathanins and phenol compounds which act as reducing, stabilization agents and that have been demonstrated to have antibacterial properties. which are compounds that help in the characterization of this plant as a natural reducing agent of remarkable efficiency [84]. Those biological active ingredients tend to reduce growth of bulk inorganic complex compounds into nanoparticles [60]. Due to their strong tendency for chelating metals, these bioactive chemicals, such as phenol compounds, function as a ligand, particle size controller, and antioxidant, bind to metal ions and reduce and cap them to form nanoparticles. This compound have a very high tendency to bind metal ions that interact with polyphenol compounds and helps in the nucleation and formation of NPs due to the presence of hydroxyl and carboxylic groups [81]. In particular, the leaves extract of *H. abyssinica* are used owing to their medicinal values and chemical constituents which helps in the reduction of toxic contents from the AgNPs [83] *H.abyssinica* leaf extracts were utilized in exchange to the chemical reagents as a potential reducing agent due to its medicinal activity. All these applications were as a result of those phytochemicals [82].

VITAMINS

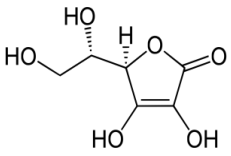

L-asrcorbic acid

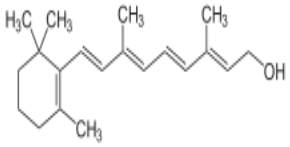

Retinol

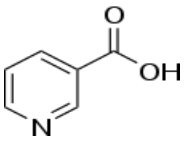

Niacin

FLAVANOIDS

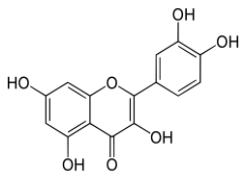

Quercetin

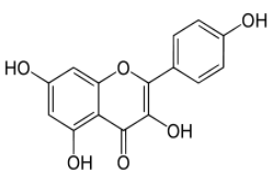

Kaempferal

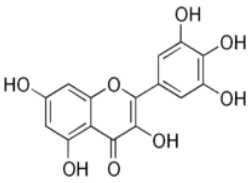

Myricetin

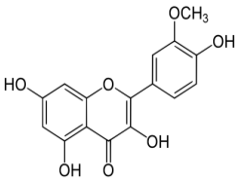

Isorhmnetin

PHENOLIC ACID

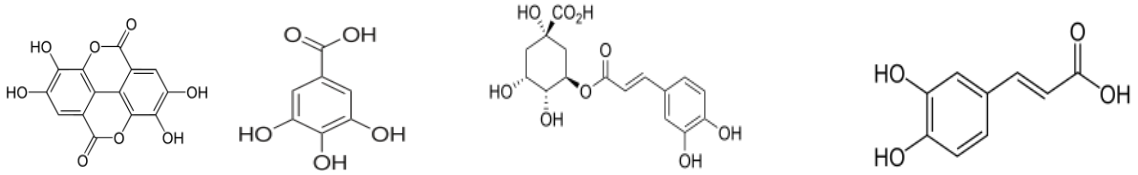

Ellagic acid Gallic acid Chlorogenic acid Caffeic

Figure 5: Schematic diagram of biological active compounds [85]

Extracts made from the leaves have strong natural antibacterial properties and some antibacterial action against gram-positive and gram-negative bacteria, according to research so far [69,79]. As it can be observed, there is a feasible alternative that allows minimizing environmental impacts, as well as obtaining better yields in the process of metal particles impregnation on a nanometric scale [60]. This extract used during the synthesis process plays an important role as it contributes/ influences the resultant nanoparticle characteristic.

In this article, we report the synthesis of Ag nanoparticles using the *H. abyssinica* natural extract as an effective capping and reducing agent. Their structural, optical, and antibacterial activity are presented.

2.7. Nanocomposite

2.7.1. Silver-Bentonite Nanocomposite

'Nanocomposites' refers to composites of more than one Gibbsian solid phase where at least one dimension is in the nanometre range and typically all solid phases are in the 1-20 nm range. The solid phases can be amorphous, semi-crystalline or crystalline or combinations thereof. They can be inorganic or organic, or both, and essentially of any composition [86].

Nanocomposites has become a very important field since such materials exhibit unexpected synergistically properties derived from components formed by combing inorganic nanoclusters, fullerenes, clays, metals, oxides or semiconductors with numerous inorganic, organic or organic polymers and organometallic compounds, biological molecules, and enzymes [87]. They can dramatically improve properties like:- electrical conductivity, decreased gas, water and hydrocarbon permeability, dimensional stability,

flame retardant, high strength, chemical resistance, thermal stability, optical clarity, surface appearance.

Nanocomposite materials synthesized by integrating nanostructured materials within the interlayer space of clay minerals have recently attracted a lot of attention due to their unusual physicochemical properties and possible applications in a variety of fields [88].

There are a limited number of studies that report the use of metal clay nanocomposite, a few studies have been conducted on the use of metal clay nanocomposite as an example copper- montmorillonite, *Guo etal*. Contemplated the adsorption properties of Cu^{2+} loaded montmorillonite (Cu- MMT) clays for *E. coli* K88. Their technique for preparation of this composite were mixing or blending and ion exchange of MMT and Cu^{2+} ($CuSO_4.5H_2O$) in solution [89]. *Bagchi et al.* synthesized copper nanoparticle based clay composite by in-situ reduction of a copper ammonium complexion. They assessed the antimicrobial action of the composite against *E. coli, S. aureus, P. aeruginosa* and *E. faecalis* [90].

Bentonite (MMT) is used as matrix for silver, in order to enlarge the clay's adsorption power and surface area; some of the studies in this area employ acidic mediums and/or high temperatures. Such routine can obviously improve the antimicrobial activity of a bentonite, but with a direct effect on the structure of the montmorillonites, which certainly affects their essential properties [92, 93].

To aggravate this problem, silver cations are very reactive and easily transformed into elementary silver by the high Ag^+ reduction power to Ag due to the poor stability of silver ions in aqueous solution after exposure to light or heat. This compromises greatly the microbiologic performance, once only ionic silver reacts over microorganisms [91]. To prevent that, some researches propose the use of chelates to stabilize the silver ions, but at more complexity and cost to the method. Researches have demonstrated bentonite intercalated with Ag^+ and other bacteriostatic beings provide a strong antimicrobial activity to the clay this since silver ion have antibacterial action and have most noteworthy antimicrobial activity.

These metals/clay composites usually prepared by ion exchange of positively charged metal ions and alkali ions present in a surface layer of clay or by synthesis of nanoparticles and immobilization them on the clay by various techniques such as ion exchange processes

and sol-gel [94,95]. Nevertheless, many of these method typically entail multiple steps combined with ultrasonication and stirring that take long hours or even days followed by chemical reduction of the precursor metal salts.

In recent years, clay mineral-based antibacterial complexes have been prepared by progression of procedures between the clay minerals and antibacterial substances. Recently, Rivera-Garza *et al.* revealed the elimination of the pathogenic microorganisms, *E. coli* and *Enterococcus faecalis* from water by silver-loaded clinoptilolite/heulandite mineral. They have been found that antibacterial action of the exchanged samples were an element of exchange level against *Pseudomonasaeruginosa* and *E. coli* [95]. In another work, a vermiculite–silver hybrid material shows strong antibacterial action against *S. aureus* [96].

The properties of natural montmorillonite and silver-composites demonstrate that the antimicrobial properties have increased [97]. Seckin and his partners have explored the antimicrobial properties of montmorillonite poly vinyl pyridinium matrix composites and reported a decrease in the number of bacterium cells in water [92].In different examinations, substitutable ions of montmorillonite were replaced by silver showed better antimicrobial properties in comparison to other metals.

2.8. Characterization Technique

2.8.1. UV-vis Spectroscopy

Ultraviolet-visible (UV-Vis) spectroscopy is one of the most popular analytical techniques because it is very versatile and able to detect nearly every molecule. UV-visible spectrometers can be used to measure the absorbance of ultra violet or visible light by a sample, either at a single wavelength or perform a scan over a range in the spectrum. The UV region ranges from 190 to 400 nm and the visible region from 400 to 800 nm. With UV-Vis spectroscopy, the UV-Vis light is passed through a sample and the transmittance of light by a sample is measured. From the transmittance (T), the absorbance can be calculated as A=-log (T). An absorbance spectrum is obtained that shows the absorbance of a compound at different wavelengths. The amount of absorbance at any wavelength is due to the chemical structure of the molecule [98].

The technique can be used both quantitatively and qualitatively. UV-Vis can be used in a qualitative manner, to identify functional groups or confirm the identity of a compound by matching the absorbance spectrum. It can also be used in a quantitative manner, as concentration of the analyte is related to the absorbance using Beer's Law. UV-Vis spectroscopy is used to quantify the amount of DNA or protein in a sample, for water analysis, and as a detector for many types of chromatography. Kinetics of chemical reactions is also measured with UV-Vis spectroscopy by taking repeated UV-Vis measurements over time. UV-Vis measurements are generally taken with a spectrophotometer. UV-Vis is also a very popular detector for other analytical techniques, such as chromatography, because it can detect many compounds.

Typically, UV-Vis is not the most sensitive spectroscopy technique, because not a lot of light is absorbed over a short path length. Other spectroscopy techniques such as fluorescence have higher sensitivity, but they are not as generally applicable, as most molecules are not fluorescent. UV-Vis has a similar sensitivity to other absorbance measurements, such as infrared spectroscopy.

2.8.2. X-ray powder diffraction analysis

X-ray powder diffraction (XRD) analysis is the most widely used technique for the identification of minerals/mineralogy analysis [99]. Identification of minerals is particularly useful for the ready determination of the nature and relative abundance of the clay minerals and other fine clay materials. The theoretical basic (*i.e*. minerals) will diffract a beam of incident pattern that characterizes each mineral species. The diffraction patterns are monitored using X-ray powder diffractometer, modem versions of which allow them to be stored and interpreted [99].

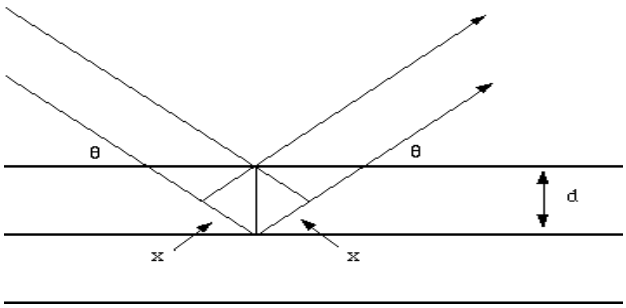

Figure 6: Principle of Bragg's equation [22]

For constructive interference between these waves, the path difference must be an integral number of wavelengths, this leads to Bragg's Equation.

$$n\lambda = 2dsin\theta \ldots\ldots\ldots\ldots\ldots\ldots\ldots\ldots\ldots\ldots\ldots\ldots\ldots\ldots\ldots\ldots\ldots\ldots\ldots\ldots\ldots\ldots\ldots (1)$$

Where n = number of wavelength(Order of Diffraction), d = the space between the planes, θ = the angle of diffraction, and λ = wavelength

It needs to be emphasized that XRD analysis can only be used to detect crystalline solids (*i.e.* minerals) present in abundances usually crystalline or 'amorphous' phases cannot be detected using this method [100].

Samples of clay materials for XRD analysis are usually prepared in two forms; a finely ground (5-10 microns) randomly oriented powder and an oriented clay (< 2µm) fraction. The finely ground whole rock powder is needed for the whole rock analysis. Apart from the identification of non-clay minerals and examination of the oriented clay fraction specimens is usually necessary for the detailed analysis of the clay minerals that are concentrated in the clay fraction. Clay fraction (<2µm) were separated by centrifuging according to Stokes Law [101]

$$V = \frac{2}{9}\,(\rho g - \rho w) g\, r^{2}/_{\eta} \ldots\ldots\ldots\ldots\ldots\ldots\ldots\ldots\ldots\ldots\ldots\ldots\ldots\ldots\ldots\ldots\ldots\ldots\ldots (2)$$

Where V = the settling velocity

ρg = density of the mineral grain (2.6 - 2.8 g/cm^3 for clay minerals)

ρw = density of water (1g/cm^3)

g = acceleration due to gravity (980 cm/sec^2)

r = radius of the mineral particle (10-4 cm for clays)

η = viscosity of water (10^{-2} gcm/sec^2)

X-ray powder diffraction (XRD) is the most widely used techniques for the characterization of Ag-NPs and Ag-Bent NC. Basically, XRD provides information

regarding the crystalline structure, nature of the phase, lattice parameters and crystalline grain size. The latter parameter is estimated by using the Scherrer's equation using the broadening of the most intense peak of an XRD measurement for a specific sample of the synthesized nanoparticles. The mean particle size (D) from XRD analysis is calculated by using Debye-Scherrer's formula.

$$D = \frac{0.89\lambda}{\Delta w \cos\theta} \ldots\ldots\ldots (3)$$

Where λ is the wave length of the incident X-ray beam (λ=1.54oA for Cu kα), θ is the Bragg's diffraction angle and Δw is the width of the X-ray pattern line at half peak height in radiance.

2.8.3. Fourier transform infrared spectroscopy(FTIR)

Fourier transformed infrared spectroscopy (FTIR) is a technique used to get the information about the chemical bonding in a material. It is used to identify the elemental constituents of a material and it helps to get structural identification and quantitative information about the synthesized nanoparticle [102]. The samples measured on spectrum 65 FT-IR (PerkinElmer) in the range 4000-400 cm-1 (resolution: 4 cm-1, number of scans:4) using /KBr pellets.

2.8.4 Atomic Absorption Spectrometry (AAS)

Atomic absorption spectrometry (AAS) is a spectro analytical procedure for the quantitative determination of chemical elements using the absorption of optical radiation (light). AAS detects elements in either liquid or solid samples through the application of characteristic wavelengths of electromagnetic radiation from a light source. Individual elements will absorb wavelengths differently, and these absorbance are measured against standards. It can be used to determine over 70 different elements in solution, or directly in solid samples via electro-thermal vaporization[103].

2.9. Antibacterial strains

S. aureus and *E. coli* account for the majority of clinical mastitis cases in cattle, whereas, *S. aureus* is the most prevalent pathogen associated with human mastitis [104]. Striking differences exist between the courses of bovine intramammary infection caused by *S. aureus* and *E. coli*. Intramammary infection by *E. coli* is acute in nature and generally clears within a few days. In contrast, infection by *S. au*reus is often less severe but results in a chronic infection that can persist for the life of the animal [105]. So, developing resistant with biocompatible application material is very important to save life from those bacteria.

The antibacterial activity of Ag-Nanoparticles, and Ag-Bentonite nanocomposite will be evaluated by agar disk diffusion technique (ADT) against gram positive (*S. aureus*) and Gram negative (*E. coli)* bacteria.

CHAPTER 3

MATERIALS AND METHODS

3.1. Materials

3.1.1 Study Sites

The raw Bentonite clay was obtained from Gewane Afar Regional State, Ethiopia and *H.abyssinica* was collected from Oromia regional state, East Arsi Zone (Qarsa town), Ethiopia. Bio –synthesis of AgNPs and Ag-Bent NCs using *H. abyssinica* plant leaf extract was carried out in the Applied Chemistry laboratory of Adama Science and Technology University (ASTU). The UV-Vis characterization and antibacterial activity were tested in the Applied Biology laboratory; XRD analysis were conducted at Materials Science Engineering laboratory, ASTU. Analysis of bentonite was conducted at Geological Survey of Ethiopia laboratory and FTIR analysis were performed at Addis Ababa University.

3.1.2 Chemicals and reagents

Source of raw Bentonite used in this study were taken from Awash Sebat of Awash region where the sample originated from Gewane Afar region Ethiopia and the *H. abyssinica* was collected from around Oromia region state, East Arsi Zone (Qarsa town), Ethiopia.

The chemicals and reagents were analytical grade and used without further purification. Silver Nitrate ($AgNO_3$) (LOBA CHEMI) was used as precursor for the synthesis of Silver Nanoparticles (Ag NPs), distilled water and ethanol (Wasse PHARMA PLC., 96-99%) was used as a synthesis medium and for washing purposes, respectively, sodium carbonate (Na_2CO_3) was used to activate Ca- bentonite, sodium pyrophosphate ($Na_4P_2O_7$) was used as precipitating agent, sodium hydroxide (NaOH) was used to adjust pH, Dimethylsulpoxide (DMSO) was used as solvent in this experiment.

3.1.3 Apparatus and Instruments

The apparatus used in the experiment were: centrifuge, hot plate, electronic balance, mechanical shaker, Whatman’s filter paper, oven, beakers (different size), Mortar and Pestle, Volumetric flask.

The instruments used were UV- Spectrophotometer (Perkin-elementary, Germany), Fourier transform Infrared spectroscopy (FTIR) (Perkin Elmer, Spectrum 65 FTIR, and USA), X-ray Powder Diffusion (XRD-700 shimadzuco, South Korea)(Cu-Kα1 radiation (λ=1.5406 A°) operating at 45 KV and 30 mA) and Atomic Absorption Spectroscopy(AAS).

3.2 Methods

3.2.1 Preparation of plant leaf extract

The leaves of *H.abyssinica* plant was surface cleaned and washed repeatedly with tap water followed by distilled water to remove dust particles and then allowed to dry under shadow for 15 days with good ventilation and in darkness to remove moisture content from the leaves. The dried leaves were ground using grinding machine and were stored in darkness in a dry place until to the next step.

The extraction was carried out by placing 20 g of powdered leaves in a beaker containing 400 ml of deionized water. Then, the beaker was covered with aluminum foil to prevent the effect of light. After that the mixture was shaken using mechanical shaker for 30 min and allowed to warm at 50 °C for 1 hr using magnetic stirrer, then it was allowed to cool down to room temperature overnight. The prepared solution was filtered through Whatman's No.1 filter paper to get clear solution. The filtrate was stored at 4 °C for further experiments [106].

3.2.2 Phytochemicals Screening on extracts from *H. abyssinica:*

The medicinal value of traditionally important plant species is due to presence of some chemical substances which produce a definite physiological action like alkaloids, tannins, flavonoids, saponins, etc [107]. To promote a proper use and our knowledge the preliminary phytochemical screening for the flowers of *H. abyssinica* were carried out to analyze the presence of compounds namely: Saponins, Anthraquinones, Flavonoids, Phenols, Alkaloids, Tannins, Terpenoids, Steroids, Phlobatannins and Glycosides.

Test for Saponins: 3 mL of the plant leaf extract was mixed with 5 mL of distilled water were added and shaken vigorously in a test-tube for about 5 min, leave to settle for 30min. Frothing (appearance of creamy miss of small bubbles) which shows the presence of saponins [108]

Test for flavonoids: To 3ml plant extract with 10 mL of ethyl acetate were mixed and heated with a steam bath for 3 min. The mixtures were filtered and 4 mL of the filtrate were shaken with 1 mL of dilute ammonia solution and a yellow coloration were observed, which shows the presence of flavonoids [109].

Test for Phenols: 2ml of plant extracts were put and treated with a few drops of 2% of $FeCl_3$ in test tube; bluish green or black coloration were indicated the presence of phenols [74].

Test for Alkaloids: 5ml of plant extract was dissolved in 10 mL of 10% ammonia solution and extracted with 15 mL of chloroform. The chloroform portion was evaporated to dryness and the resultant residue dissolved in 15 mL of dilute sulphuric acid. . Reddish brown color was formed which showed the presence of alkaloids [108].

Test for Tannins: A few drops of 10% ferric chloride ($FeCl_3$) solution were added to 2 mL of the aqueous solution of the plant leaf extract. The occurrence of blackish blue color showed the presence of tannins [109].

Test for Terpenoids: 0.5 g of each crude powders were separately dissolved in 5 mL of methanol. 2 mL of the extract were treated with 1 mL of 2, 4- dinitrophenyl hydrazine were dissolved in 100 mL of 2M HCl. Yellow-orange colorations were observed as an indication of Terpenoids [74].

Test for Steroids: 3ml of plant extracts were dissolved in 5 mL of methanol. 1 mL of the extract were treated with 0.5 mL of acetic acid anhydride and cooled in ice. This mixed with 0.5 mL of chloroform and 1 mL of concentrated sulphuric acid was then added carefully by means of a pipette. At the separations level of the two liquids, reddish-brown rings were formed, as indication of the presence of steroids [83].

Test for Phlobatannins: 2 mL of plant extracts were added to 2 mL of 1% HCl and the mixture was boiled. Deposition of a red precipitates were taken as an evidence for the presence of phlobatannins [83] ,but the yellow precipitate was form which indicates zero presence of phlobatannin.

3.2.3 Green Synthesis of Ag NPs

The Ag nanoparticles were synthesized using different volumes ratios of 0.2 M $AgNO_3$ solution with leaf extract prepared from 20 g in 400 ml distilled water. First 100 ml of plant leaf extract was mixed with 100 ml of 0.2 M $AgNO_3$ solution (1:1), next 200 ml of 0.2 M $AgNO_3$ solution and 400 ml leaf extract solution (1:2), followed by adding drop wise 100 ml of 0.2M $AgNO_3$ solution with constant stirring to 400 ml of leaf extract (1:4) at the temperature of 50 °C. The solution pH was adjusted to pH 12 by drop wise addition of 1M NaOH. The mixture has been incubated in dark chamber to minimize photo-activation of silver nitrate at room temperature until a color change observed. Then, the solution was centrifuged for 15 min at 10000 rpm, the obtained Ag-NPs (Figure 7) was filtered by Whatman's No#1 and washed by deionized water and ethanol to remove impurities. Thereafter, the NPs was allowed to dry and ground so as to be used for further analysis [82].

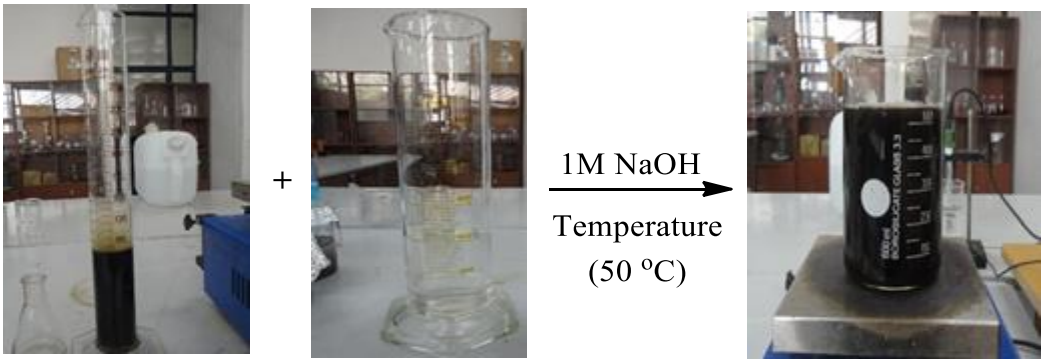

Figure 7: Image for the synthesis of Ag NPs.

The colorless solution changed to dark brown which indicates the formation of Silver Nanoparticles (AgNPs). The formation of the AgNPs during the reduction process is indicated by change in the color observed with different time interval 0min, 15min, 30min and 1hr, respectively from colorless to dark brown within reaction duration.

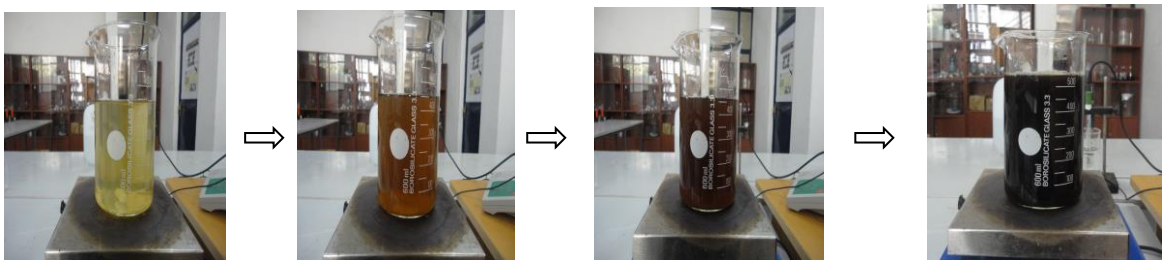

Figure 8: Change in the color observed during AgNPs Synthesis

3.2.4 Purification of Bentonite

Primarily sand fraction (> 75μm) were removed by wet sieve then the clay fraction was separated from silt by centrifugation of sedimentation from suspension according to Stokes law. The suspension pass through 75μm IS sieve (clay and silt) were stirred for more than 30 min with addition of 0.0005 mol/l sodium pyrophosphate as deflocculating agent then the suspension transferred in to large cylinder to settle. According to Stokes low clay particles settle in a velocity of 902D2 mm/sec (where D is the diameter of the clay particle)[100], then the distance on the cylinder was measured and the amount of water was poured off and collected then filtered to separate the clay fraction from water and left to dry.

3.2.5 Activation of Bentonite

The bentonite sample was activated by sodium carbonate (Na_2CO_3) according to *N. Yildizet al* [110]. The soda (Na_2CO_3) with the mass 5g and 100g of bentonite sample were added to 500 ml of boiling water. The suspension was stirred slowly and continuously with a magnetic stirrer and was boiled for 1 hr at 50^oC. After activation, it was allowed to cool down at room temperature and was diluted with more distilled water .The diluted suspension was dispersed homogeneously and allowed to stand for 24 hrs to settle the impurities, especially quartz. After 24 hrs, the supernatant was decanted and the sedimentation process was repeated until the supernatant became clear. The collected supernatants were centrifuged at 10000 rpm to 20 min to settle the clay sample and dried at 60^oC to obtain the activated bentonite. The dried sample was further ground to obtain fine powder for further experiment [111].

3.2.6 Synthesis of Ag-Bentonite Nanocomposite

The preparation of Ag-Bentonite composite were carried out as follow: in two different beakers with 100 ml distilled water 3g of activated Bentonite were added to prepare bentonite suspensions, and 100 ml solution of 0.1M and 0.2M of $AgNO_3$ were separately added to each beaker and stirred for 24 hrs at room temperature, followed by adding fresh 200ml and 400ml of leaf extract respectively, to obtain the dark brown $AgNO_3$/Bent suspensions through vigorously stirring on magnetic stirrer for 1 hr at a temperature of 60-^oC. The suspensions of Ag/Bent NCs obtained were then centrifuged at 15,000 rpm for 5

minutes, and the precipitates washed 4 times using distilled water in order to remove the silver ion and other residues, and dried overnight at 40°C under vacuum [112].

3.2.7 Characterization methods

3.2.7.1 XRD Spectroscopy

Analysis of the crystal phases and average crystalline size analysis of the synthesized Ag-NPs and Ag-Bent prepared through green method using *H. abyssinica* leaf extract was done with an X-ray diffractometer. X-ray diffraction (XRD-700 shimadzuco, South Korea) was performed with 2θ ranges from 10° to 80° (Bragg angles) for AgNP and 0º to 80º for Ag-Bent NCs with Ni-filtered Cu Kα radiation of 0.1540 nm (λ=1.54Å), with scan rate 1.5º/min(2° min $^{-1}$) 3 (deg/min), a working voltage of about 40 kV, and a working current of about 30 mA. The powder samples were mounted into a top-loaded circular sample holder to be rotated in the instrument at 50 rpm.

3.2.7.2 UV-Visible Spectroscopy

For the electronic absorption measurements and Optical properties of *H. abyssinica* leaf extract based green synthesized Ag-NPs and Ag-Bent NC were determined by UV–Vis spectroscopy (SM-1600 Dual beam UV-VIS Spectrometer, Azzota Corp., USA). 3 mL solution of Ag-NPs and Ag-Bent was taken in a cuvette and scanned using double beam UV-Vis-spectrophotometry from 200 nm to 800 nm wavelengths and their maximum absorbance was recorded.

3.2.7.3 FTIR Spectroscopy

The functional group present in AgNPs and Ag-Bent NCs were analyzed by the Perkin Elmer Spectrum 65 Spectrum BX FTIR (at Addis Ababa University, Department of chemistry, Ethiopia). A portion of the prepared samples were pulverized to a fine powder in an agate mortar and pestle. A small portion of the material weighing approximately 2 mg was then ground and mixed thoroughly with 40 mg of dried potassium bromide (KBr). The powder was distributed evenly within the die by first rotating the plunger, and the assembly was placed in a press. The die was disassembled and the KBr disc carefully removed and placed in a sample holder. The beam splitters used were KBr for the mid-IR region 4000 to 400 cm^{-1} and the resolution was 4 cm^{-1}.

3.2.8 Atomic absorption analysis of Bentonite

The Raw bentonite and Na-activated bentonite samples were characterized by using AAS to determine their chemical composition. For complete silicate analysis of both samples 0.1 gram of each was added separately to 1.5 g of lithium boron oxide ($LiBO_2$) and the mixtures was heated in a furnace for 45min at 950°C. After they were cooled overnight, the mixtures were stirred by a magnetic stirrer, washed and transferred to round bottom flasks with addition of lanthanum chloride ($LaCl_3$). The prepared solutions were used to determine metals like Ca, K, Al, K, Mg, Fe, Na, etc. The amount of silica was determined by taking 0.1g each samples, 3mL of HCl and 2 mL of boric acid directly read by the instrument and the amount of TiO_2 and P_2O_5 was determined by UV-Vis spectrophotometer[113].

The Raw bentonite chemical compositions analysis using atomic absorption spectrometer before activation results indicated in Table 1 below.

Table 1. Chemical analysis of the raw bentonite sample.

Code	**SiO_2**	**Al_2O_5**	**Fe_2O_3**	**CaO**	**MgO**	**Na_2O**	**K_2O**	**P_2O_3**	**TiO_3**	**H_2O**	**LOI**
%	55.50	12.64	7.70	3.10	2.5	1.38	0.97	0.64	0.35	4.38	9.8

3.2.9 Antibacterial Activity

3.2.9.1 Disc Diffusion Method

In vitro antibacterial susceptibility test was determined by disc diffusion method against the bacterial species representing Gram negatives (*E. coil*) and Gram positives (*S. aureus*). The medium was prepared by dissolving 38 g of Mueller Hinton agar medium in 1000 mL of distilled water and autoclaved at 121 °C for 15 min. The autoclaved medium was poured into sterile plates (20-25 mL/plate) and the plates were allowed to solidify under sterile condition at room temperature. After solidification, the plates were seeded with overnight grown culture approximately 1.5 X 10^8 CFU/mL (McFarland standard) by swabbing evenly on to the surface of the medium with a sterile cotton swab.

Ag NPs and Ag-Bent NCs at the concentrations of 125µg/mL were prepared by dissolving in DMSO. Whatman's filter paper No. 1 was used to prepare discs approximately 6 mm in diameter. The sterile discs were infused with AgNP and Ag-Bent NCs and position on the surface of the medium with sterile forceps and gently pressed down to ensure contact with the MHA. Ciprofloxacin (as control positive)] was used as standard antibiotic and then plates were inverted and then incubated at 37^0C for 24 hrs. After incubation the inhibition zone produced by Ag NPs and Ag-Bent NCs were evaluated by measuring the diameter (mm) of the clear zone around the disc against the test organisms using a ruler [114].

Also the antibacterial activity of Raw Bentonite (unpurified), Ca-Bentonite (purified) and Na-Activated Bentonite was tested against gram negative and gram-positive bacteria strains of *E.coli* and *S.aureus* respectively, using this method.

CHAPTER 4

RESULT AND DISCUSSION

4.1. Phytochemical screening of *Hagenia abyssinica* plant leaf extracts result

H. abyssinica plant extracts were rich in different phytochemicals with different functional groups, which acts as a natural stabilizer. These phytochemicals were revealed to be present in extracts of *H. abyssinica* which are known to have antimicrobial activity and the results are in good agreement with a previous report [115].

Table 2: Phytochemical screening of the *H. abyssinica* plant leaves aqueous extracts.

Phytochemical Constituent	Observation	Result
Saponins	A foam /frothing/	+
Flavonoids	Yellow color	+
Phenols	Bluish green	+
Alkaloids	Reddish Brown color	+
Tannins	Brownish greens	+
Terpenoids	Yellow color	+
Phlobatannins	Greenish yellow	_

+ = the presence of phytochemical constituents - = the absence of phytochemical constituents

The present study demonstrates that *Hagenia abyssinica* is a good source of various phytochemical such as Saponins, Flavonoids, Phenols, Terpenoids, Alkaloids, and Tannins that can be used for reducing silver ion to silver metal and as a capping agent to prevent agglomeration of the silver nanoparticles.

4.2 Activation of Bentonite Analysis

Table 6 shows the major elemental silicate analysis of sodium activated samples. The compositions of activated bentonite with Na_2CO_3 that Ca^{2+} ions were exchanged by Na^+ ions where Na_2O became 5.90 % from 1.41 % when 5% of Na_2CO_3 was added, but the CaO content decreased the percentage changed from 3.15 to <0.01, indicating that Ca^{2+} has been replaced by Na^+ in MMT. This is because divalent ions like Ca^{2+} have been replaced by Na^+[116]. Hence, Na^+ smectite clay is one of the preferred layered materials for the preparation of nanocomposites because of its high cation exchange capacity, high surface area, strong adsorption /absorption capacities within their interlamellar spaces and thus swelling capacity[113].

The increment of H_2O percentage is related to the activation. Because the swelling capacity of Na-bentonite was greater due to the location of Na+ in between the Octahedral and Tetrahedral layer, water could hydrate in the clay mineral due to weak electrostatic interaction between the sodium ion and the negatively charged smectite layer, allowing excess water molecules to enter. Smaller ions tend to have greater hydration energies, and thus within the interlayer of clays can attract more water than large ions. The degree of attraction to the clay surface of Na^+ is less, so a Na^+ is more conductive to swelling when present at the clay surface, because adjacent negatively charged layers can be made to repel one another during the absorption of water into the interlayer. On the other hand, Ca^{2+} saturation results in only limited swelling because the attraction of the cation for adjacent surface is stronger[116]. Ca ions of the samples are replaced by Na ions.

The result for the rest of chemical compositions shows; decrease of SiO_2 and Al_2O_3 after Na_2CO_3, activation, followed by sedimentation, confirmed the removal of minor amount of quartz impurity and the proportional increase of the clay mineral content. In contrast the MgO content remained unaffected. The percentage of Fe_2O_3, K_2O and CaO is also decreased but Small amounts of Fe_2O_3, K_2O and CaO were still present in the purified sample. The K_2O is most probably due to illite and CaO to trace amounts of calcite and/or feldspar. The studied bentonite clay was free of the toxic trace elements Pb and As, since the concentrations of both elements were below the detection limit of ICP-AES (0.05 ppm and 0.01 ppm for As and Pb respectively)[111].

Table 3: Chemical analysis (AAS Analysis) of bentonite after sodium activation

Oxides %	SiO_2	Al_2O_3	Fe_2O_3	CaO	MgO	Na_2O	K_2O	P_2O_5	TiO_2	H_2O	LOI
Raw	55.50	12.64	7.70	3.10	2.5	1.38	0.97	0.64	0.35	4.38	9.8
5%Na-bent	55.15	12.20	6.86	<0.01	2.5	5.90	0.94	0.55	0.36	5.31	8.8

4.3 Characterization of Synthesized Ag-NPs and Ag-Bent NCs

4.3.1 X-ray Diffraction (XRD) Analysis

X-ray diffraction (XRD) was used to evaluate the phase purity and crystallinity of the produced AgNPs and Ag-Bent NCs. According to the XRD pattern, the product is mostly composed of Silver (Ag) in Silver Nanoparticles (AgNPs) peaks and bentonite and Ag in Ag-Bent NC peaks. Diffraction peaks for Ag NPs (Figure 9) are seen at 2θ values of 38.074°, 44.365°, 64.485°, and 77.424°, corresponding to (hkl) values of (111), (200), (220), and (311) Bragg's reflections for AgNPs, which are comparable and are evident in all patterns, which are previously reported by *H. Bar et,al* [117] and suggest that the synthesized AgNPs using aqueous extract of *H. abyssinica* leaves is found to possess a FCC structure which were in good agreement with reference to the unit cell of FCC structure of silver nano-crystals (Joint Committee on Powder Diffraction Standards: File No. 04-0783) [118].

The increase in phytochemical in the higher concentration of *H. abyssinica* reduce the silver ion and helps in the formation of small particles which gives intense surface plasmon resonance [83]. The high intense peak for FCC materials is generally (111) reflection, which is observed in the sample. The intensity of peaks reflected the high degree of crystallinity of the silver nanoparticles. However, the diffraction peaks are broad which indicating that the crystallite size is very small [119]. The XRD shows that silver nanoparticles formed are crystalline. The average particle size of synthesized AgNPs is calculated from FWHM of the diffraction peaks using Debye-Scherrer equation. The size of the Ag nanoparticles estimated from the Debye–Scherrer formula are 1:1, 1:2 and 1:4 with size of 23.05, 22.99 and 21.76 nm, respectively. The results clearly show that biomolecules present in the leaf extract reduced and capped silver ions to silver nanoparticles in a bio-synthesis process. The XRD pattern thus clearly shows that the

silver nanoparticles formed by the reduction of Ag^{+} ion by *H. abyssinica* leaf broth are crystalline in nature. The unassigned peaks, marked with # at 2θ = 27.75 °, 32.20 ° and 46.2 ° in Figure 9 could be due to the crystallization of bioorganic phase that occur on the surface of the silver nanoparticles and also are thought to be related to crystalline and amorphous organic phase[120]

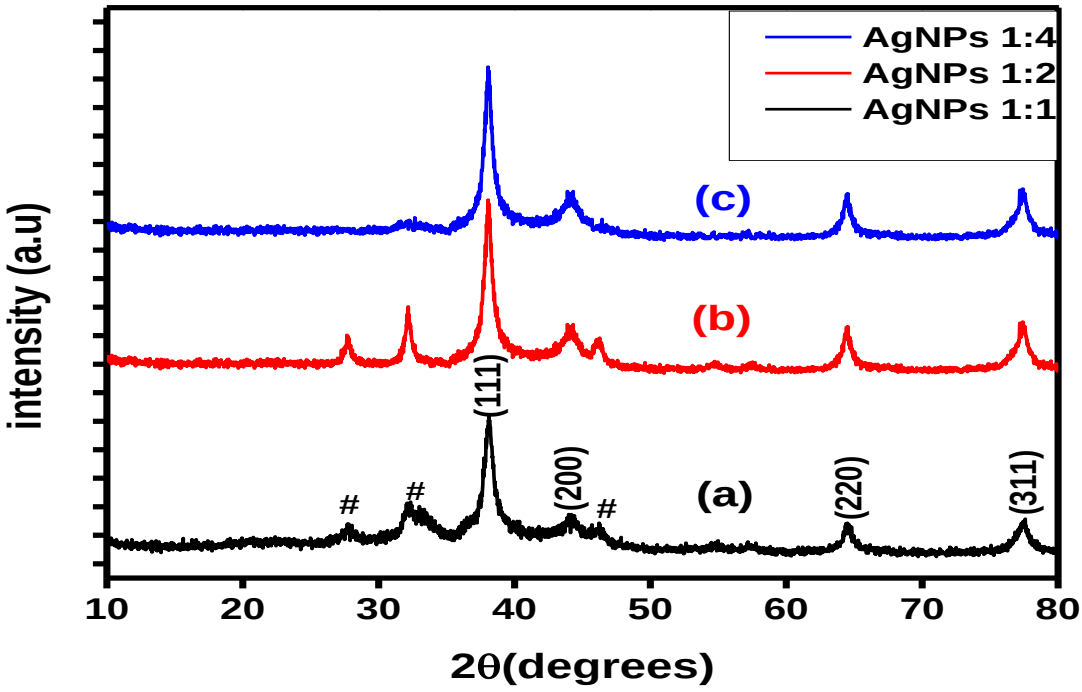

Figure 9: XRD Patterns of the AgNPs

The average particle size of different $AgNO_3$ and *H. abyssinica leaf* extract ratio 1:1,1:2 and 1:4 was found to be 23.05 nm, 22.99 nm and 21.76 nm which was derived from the FWHM of more intense peak corresponding to 111, 200, 220 and 311 using Scherrer's formula. The difference in size could be due to the effect of the volume of plant extract on AgNPs [121].

This result confirms AgNPs 1:4 that the capped nanomaterial by the plant extract has a smaller particle size than AgNP 1:1 and 1:2, as the concentration of plant leaf extract increases the particle size decreases. This was due to the fact that the greater amount of the plant extract used during the synthesis process results in effective capping and stabilizing the synthesized nanoparticles and hindered from aggregation. Therefore, the crystallinity of AgNPs prepared using high volume of plant extract is better.

Table 4 also shows that the average crystal size of AgNPs synthesized by using 1:4 ratios by volume of precursor salt and plant extract was less than their corresponding to the other two ratios. This may also be due to the high concentrations of bio-molecules from plants that present in the NPs that could highly stabilize the nanoparticles by capping and hinders further crystal growth [83].

Table 4: The crystalline size, lattice parameter value of biosynthesized Ag NPs peaks

Sample in ratio	Peak position(2θ)	FWHM	Size of NPs(nm)	Average size(nm)	d-spacing (nm)	hkl
AgNPs 1:1	38.07	0.31206	26.93	23.05	2.36	111
	44.02	0.43909	19.51		2.06	200
	64.46	0.47474	19.78		1.45	220
	77.36	0.39182	25.97		1.23	311
AgNPs 1:2	38.12	0.4353	19.79	22.99	2.36	111
	44.02	0.33345	25.78		2.06	200
	64.49	0.39564	23.74		1.44	220
	77.40	0.45076	22.63		1.23	311
AgNPs 1:4	38.10	0.3600	23.6	21.76	2.36	111
	44.12	0.600	14		2.04	200
	64.44	0.600	20.36		1.44	220
	77.34	0.5200	29.12		1.23	311

4.3.1.1 XRD analysis for Activated Bentonite

The XRD characterization of the clay samples aimed to confirm the presence of associated minerals and clay minerals. Figure 10 presents the x-ray diffraction results of activated bentonite clay which shows the diffraction peaks at around the angles 15.81 º, 19.80 º, 26.42 º, 30.61 º, 34.68 º, 37.17 º and 61.4 ° which corresponds to the crystal planes of (211), (220), (400), (332), (431), (440) and (842) as majority phases. The inter-planar distance calculated according to Bragg equation: $2d\sin\theta = \lambda$. Impurities such as kaolinite and quartz were found in the XRD patterns of the bentonite clays obtained in this study. . Similar XRD results were obtained when they performed the characterization of bentonite clay by *Muhammad et al* [122]. In the clay composition, the characteristic peaks of montmorillonite (M), gypsum (G), and kaolonite (K) were presented in Figure 10 table 4.

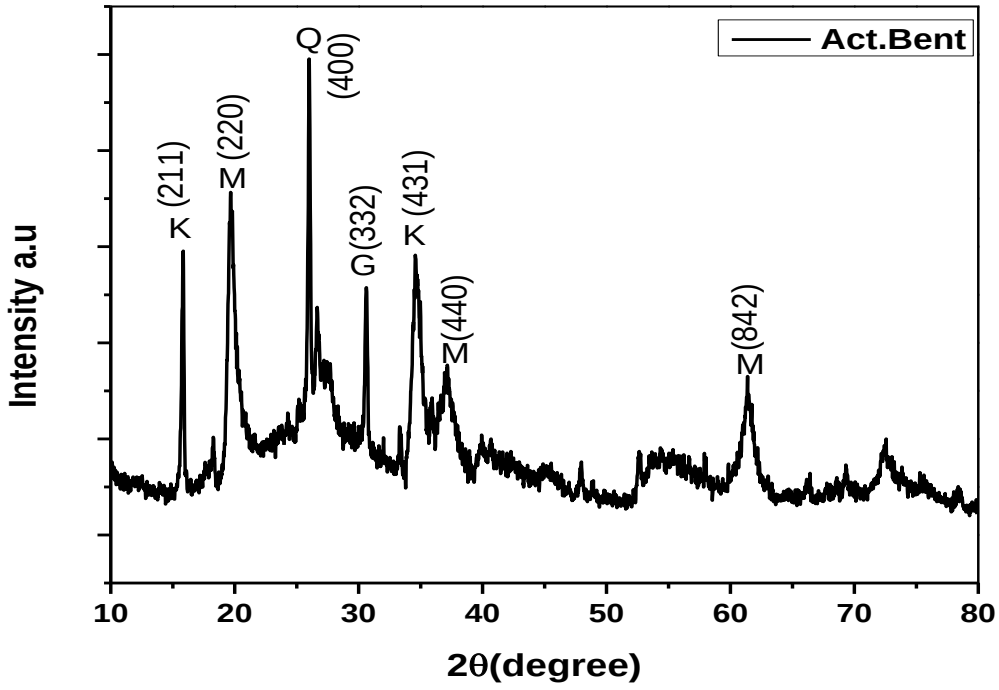

Figure 10: XRD result of Activated Bentonite

Table 5: XRD result for Activated Bentonite

Peak position(2θ)	Miller index	Reflection	d-spacing(d(nm))
15.81	(211)	Kaolinte(K)	5.61
19.80	(220)	MMT(M)	4.48
26.42	(400)	Quartz(Q)	3.37
30.61	(332)	Gpysum(G)	2.92
34.68	(431)	Kaolinte(K)	2.59
37.17	(440)	MMT(M)	2.42
61.48	(842)	MMT(M)	1.51

4.3.1.2 XRD analysis for Ag-Bent NCs

The XRD pattern were employed to determine reflections of activated bentonite and Ag^{+}-exchanged bentonite in the AgNP-Bentonite, which bentonite is the predominant clay component in the sample, and to mineral admixture such as quartz, kaoline and gypsum. The existence of silver nanoparticles was verified by the XRD pattern after nanoparticles of Ag were deposited on the clay, peaks are observed corresponding to the formation Ag in the composites at 2θ values of 38.08°, 44.42°, 64.40° and 77.84°, corresponding to the reflections of crystallographic planes (111), (200), (220) and (311) plane, which confirm the face centered cubic (fcc) crystal structure with the major peaks. The results were consistent with the data in ICPD file No. 00-004-7383. (Fm3m). Figure 11 also shows the XRD patterns of bentonite in which the diffraction peaks are at $2\theta \sim 8.6^{o}$, 15.8^{o}, , 20.08^{o}, 26.04^{o}, 29.42°, 30.68°, 34.74^{o} corresponds to (001), (211), (220), (400), (330), (332), (431) planes are due to the silicate unit. With increasing Ag NPs in the solid support matrix, the intensities of (111), (200), (220), and (311) reflections owing to the Ag NPs phase also increased [123]. The presence of the diffraction patterns of Ag and bentonite confirms that the prepared composites are composed of these two species.

As the concentration of Ag precursor decreases, the AgNPs distinctive peaks found in Ag-bentonite NCs also decreased. As a result, the Ag characteristics peak intensity in Ag-bentonite NCs is lower in Ag-bentonite NCs (0.1M) than that of Ag-bentonite NCs (0.2M). It's observed that the intensity of Ag characteristic peaks in Ag-bentonite NCs (0.1M) is weak compared to Ag-Bent NCs (0.2M). The capacity of Ag to connect nearby silicate units between layers accounts for the broadening of the peaks. The left hand peaks (below 2θ of 30^{o}) strongly show the bentonite character, while the right hand peaks (above 2θ of 30^{o}) strongly show the Ag character, which are compressed as a result of Ag bridged the neighboring silicate units of bentonite in XRD spectra of all Ag-bentonite NCs.

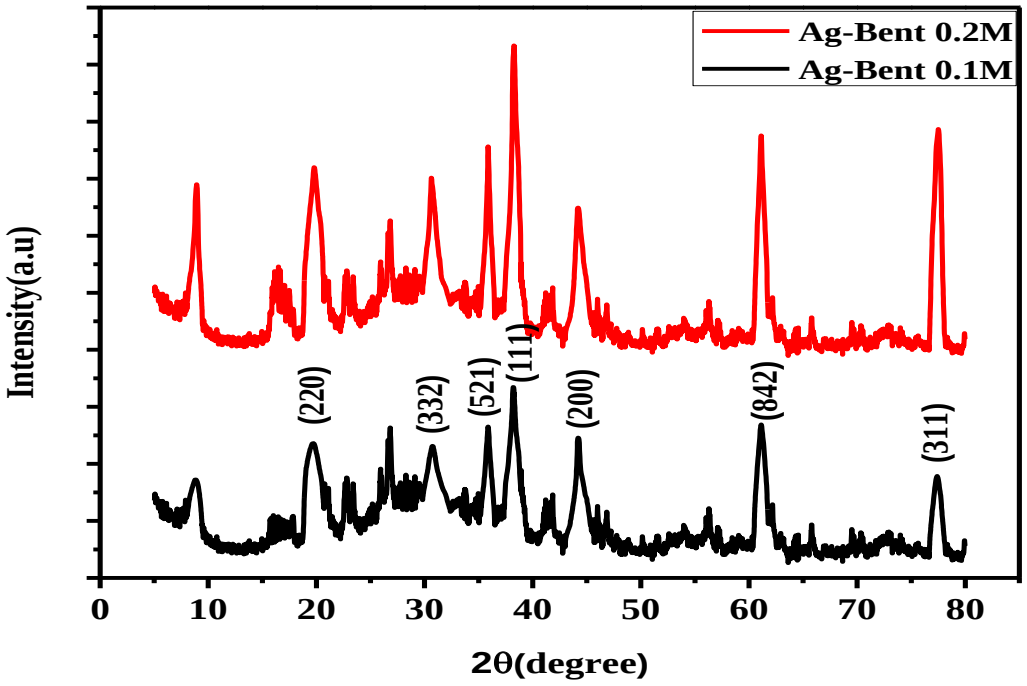

Figure 11: XRD patterns of the Ag-Bent NCs

The XRD pattern of Ag-bentonite clearly shows that in the presence of a high concentration of Ag solution (0.2M), the composite characteristics peak intensity and interlayer spacing value increase, whereas the composite characteristics peak intensity and interlayer spacing value decrease in Ag-bentonite NCs with a low concentration of Ag solution (0.1M). However, decreasing amount of Ag content is accompanied with formation of smaller size NCs. This might be due to more enough amount of bentonite clay responsible for capping and preventing AgNPs from agglomeration. For the smaller particles the peak broadening are larger and some of the peaks begin to overlap to a rather

large extend. As the particles become smaller the signal also gets weaker. In general, it is clear from XRD data analysis of Ag-bentonite NCs that increase in the number of Ag samples led to increased reflection intensity and narrowing. Recrystallization and continued development of Ag crystallites produce an increase in intensity and narrowing, as have shown (Figure 11). The XRD patterns of Ag-Bent NCs revealed no diffraction peaks related to contaminants, demonstrating the great purity of the produced products.

The average diameter of crystallites (D) is calculated by using Debye-Scherer equation.

Inter-planar d-spacing was also calculated using Bragg's Law equation (Table 5):

$2d \sin\theta = n\lambda$, Where, θ is Bragg's angle of diffraction and $n= 1$.

Table 6: Average particle size and inter-planar d-spacing for the major peaks of Ag-bentonite NCs and bentonite.

Sample	Peak 2θ(°)	β (rad)	D (nm)	Average (nm)	d(nm)
Ag-Bent (0.1M)	38.06	0.9800	9.59	10.70	2.35
	44.13	0.8717	10.30		2.05
	77.37	0.8906	12.23		1.23
Ag-Bent (0.2M)	38.13	0.9100	9.65	10.34	2.36
	44.20	0.8873	10.18		2.05
	77.52	0.9523	11.21		1.23

4.3.2 UV-Vis Analysais

UV-Vis spectrophotometer is useful in characterization and can provide certain information about shape, size, and stability of nanoparticles. The plasmonic absorbance phenomenon of nanoparticles makes it detectable by UV-Vis spectrophotometer [124].

4.3.2.1 UV-Vis for AgNPs

The UV–visible absorption spectra of Ag nanoparticles synthesized at different concentrations of leaf extract with 0.2M of $AgNO_3$ at 1:1, 1:2 and 1:4 were recorded and analyzed by UV spectra of Plasmon resonance band at 410 nm, 419 nm and 423 nm respectively in Figure 12. This absorption bands are basically due to a surface Plasmon resonance of Ag NPs, consistent with previous reports of peak in the absorption spectrum of 400-500 nm due to SPR in AgNPs [125]. The formation of the AgNPs during the reduction process is indicated by change in the color of the reaction solution from colorless to dark brown within reaction duration. The appearance of the brown color and of the peaks was due to the excitation of the Surface Plasmon Resonance (SPR), Maximum absorbance at 423 nm was observed, similar characteristic property of silver nanoparticle reported by *Shakeel Ahmed al et* [106]. Metal nanoparticles have free electrons, which yield a surface plasmon resonance (SPR) absorption band, due to the mutual vibration of electrons of metal nanoparticles, when they align in resonance with light. A single SPR band is expected in the absorption spectra of spherical metal nanoparticles, whereas anisotropic particles could give rise to two or more SPR bands depending on the shape of the particles [126]. In this case, a single SPR band is observed, which leads one to predict that the particles are spherical in shape. If we increase the leaf extract concentration, there is increase in wavelength from 410 nm up to 423 nm as presented in Figure12. On increasing concentration of extract there is increase in intensity of absorption. The slight variation in the values of absorbance signifies that the changes are the particle size. In this study, a single SPR band is exhibited, which shows no agglomeration of AgNPs [127]

The peak position of UV-visible spectra are related to nanoparticle size, with blue shifted or moved to lower wavelength or greater energy as nanoparticle crystal size decreased [128]. The blue shift (hypsochromic shift) occurs due to reduction in the size of particles from large size to small size. Further increase in extract volume resulted in a substantial broadening of absorbance peak. There is also a disappearance of broadening. Broadening

and a red shift are attributed to agglomeration or increase in size of the particles [128]. This might be due to the increase in absorbance could be attributed to the larger particle size of AgNPs. In this study, increasing the volume of the plant extract was used to optimize the size of the AgNPs synthesized. A decrease in particle size was observed when increasing the volume of plant extract. Organic reducing and capping agents are present in various concentration in different volumes of extracts. This suggests that at larger extract concentrations, the biomolecules function as a reducing agent, capping the nanoparticle surfaces and preventing aggregation. The flavonoids and terpenoids present in *H. abyssinica* extract act like natural reducing agent which is responsible for reducing silver to silver nanoparticle. The UV-vis spectra recorded, implied that most rapid bio reduction was achieved using *H. abyssinica* leaf extract as reducing agent [129].

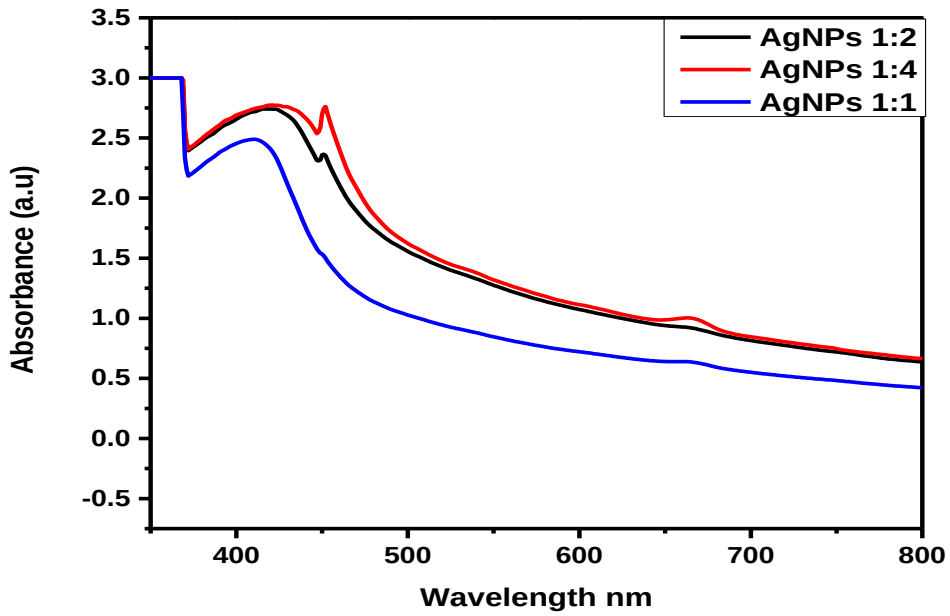

Figure 12: UV-Vis spectra of AgNPs and Ag-Bent NCs

4.3.2.2 UV-Vis for Ag-Bent NC

The UV-Vis absorption spectra of Act-bentonite and Ag-Bent NCs are shown in Figure13. The UV-Vis spectrum of AgNPs (1:4) and Act-bentonite shows an absorption peak at approximately 430 nm and 364 nm, respectively. Ag-Bent NCs has two different peak that indicative of the formation of a fine layer of AgNPs on the Bentonite.

The result indicates that particles with smaller diameters are synthesized at higher leaf extract concentrations, which favors the adsorption of nanoparticles on the clay's surface. This reduction shows that a possible greater adsorption of clay nanoparticles occurred because there was no colloid agglomeration and the particles formed presented smaller diameter. Ag remains synthesized on solid phase (MMT) during the process of its reduction to metallic Ag, while Ag ions are removed from the interlayer and then reduced and adsorbed on the outer surface and edges of the clay[130].

After the ion exchange process, the intensity of the absorbance bands of AgNPs with the ratio of 1:4 and bentonite decreases. The peak of the AgNPs shifts a red shift from 430nm to 488nm and the bentonite peak shifts from 364nm to 368nm. The absorption spectra also indicated that the intercalated AgNPs formed between adjacent MMT lamellar layers were smaller, but that most of the Ag NPs were formed at the MMT suspension interface. The $AgNO_3$ / Bent was colorless, but after the addition of the leaf extract to the suspensions, they turned brown and dark brown, indicating the formation of Ag NPs in the bentonite suspensions. The formation of Ag NPs was also followed by measuring the surface plasmon resonance (SPR) bands of the Ag-Bent NCs suspensions at a wavelength of 300–700 nm [112]. The absorption peak due to SPR of Ag was slightly red-shifted to higher wavelength, which indicated the increase in the size of Ag NPs. The absorption peak for 0.2M of $AgNO_3$ was considerably increased and was red-shifted to 368 nm. Higher concentration of metal nanoparticles may also lead to the red-shift of SPR band [32].

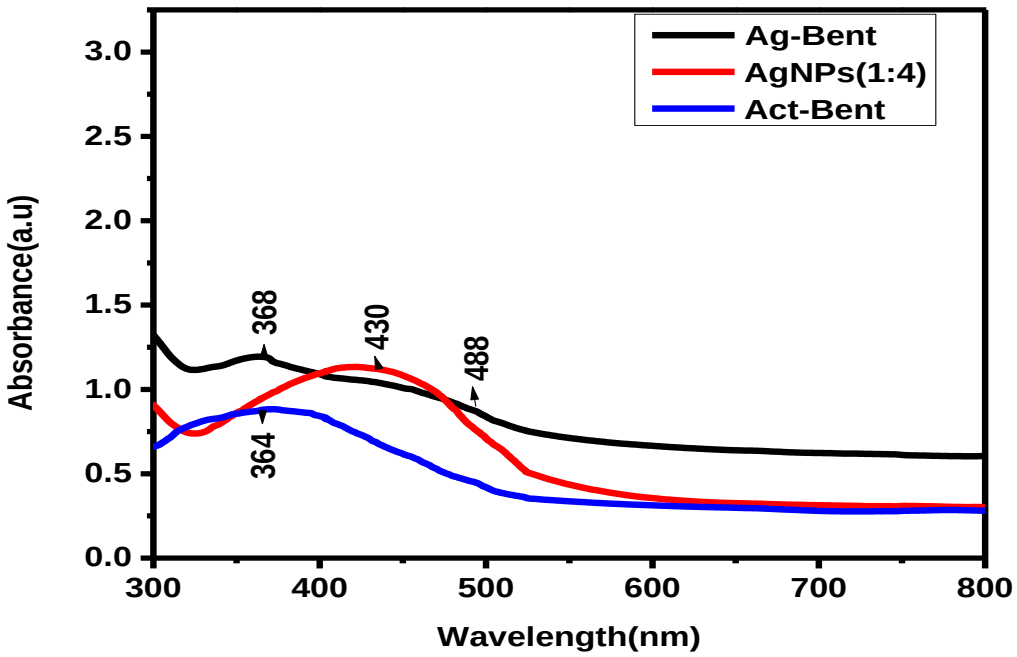

Figure 13: UV-Vis absorption spectra of Ag NPs, bentonite and Ag-bentonite NCs.

4.3.3 FT-IR Spectra Analysis

Figure 14 shows the FTIR spectra of activated bentonite indicates that montmorillonite is the dominant mineral phase in bentonite. The montmorillonite presented bands in the region of approximately at 3557 cm^{-1} is due to stretching vibrations of structural OH groups (hydroxyl group) of montmorillonite and a broad band at 3424 cm^{-1} of the OH stretching vibration and structural adsorbed water, coordinated to octahedral Al^{3+} cations.

In the lower frequency region, montmorillonite had a strong band at 1020 cm^{-1} bonding to the Si–O stretching vibration of bentonite mineral. The absorption band at 1635 cm^{-1} was attributed to the OH deformation mode of water. The clay spectrum also contains a band in the region 600-800 cm^{-1} which indicated the presence of quartz. In addition the peaks at 461cm^{-1} angular Si-O-Si vibrations and 523 cm^{-1} band is related to the angular Si-OH-Al (octahedral layers of aluminosilicates) vibration in the bentonite [131].

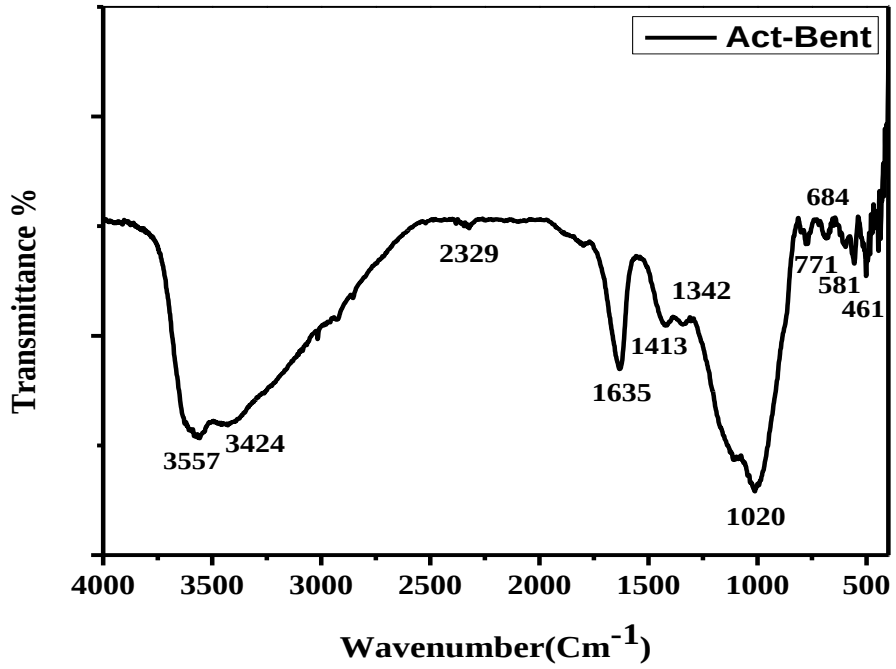

Figure 14: FTIR spectra of Activated Bentonite

Figure 15 shows the FT-IR spectra of the optimized AgNPs (1:4) and Ag-Bent NCs (0.2M, 1:4). The common spectrum absorption peaks detected at around 3559 cm^{-1}, 3438 cm^{-1}, and 1635 cm^{-1} on the surface of nanomaterials indicate typical stretching vibration of the hydroxyl functional group (O-H), stretching vibration of C-H, and bending vibration of O-H, respectively. The stretching vibration of the C=C group was also found in the 1610-1680 cm^{-1} range [132].The bonds or functional groups such as –C–O–C–, –C–O, and –C=C– derived from heterocyclic compounds, e.g., alkaloid or flavones and the amide (I) bond derived from the proteins that are present in the leaves extract are the capping ligands of the nanoparticles. The peaks belong to carbonyl, alcohol, and nitro functional groups confirms the presence of alkaloid, phenol, terpenoids, polysaccharides and flavonoid present in the *H. abyssinica* leaves extract which is responsible for the reduction of Ag^{+} ions to AgNPs. These functional groups have been observed on the surface of AgNPs produced from leaf extracts [133]. The wide and strong bands at 3559–2925 cm1 were caused by bonded hydroxyl (–OH) or amine groups (–NH) in the *H. abyssinica* extract, as well as aliphatic C–H. The carboxyl group (C=O) stretching vibrations are responsible for the peak at 1635 cm^{-1} [134]. The peak at 1020 cm^{-1} is due to Ag-NP banding with oxygen

from hydroxyl group of *H. abyssinica* compound. The vibration bands in the 3559 cm^{-1} area related to O–H stretching, whereas 3438 cm^{-1} the interlayer O–H stretching (H bonding), 1635 cm^{-1} corresponded to H–O–H bending. In contrast, these peaks were either absent or displayed drastically reduced intensities in the corresponding silver nanoparticle spectra. This seems to suggest that functional groups in this region are involved in the reduction and stabilization of the AgNPs by their subsequent oxidation. Additionally, ether linkages, C–O and C–O–C functional groups are thought to be groups of flavones, terpenoids and polysaccharides present in *H. abyssinica* leaf extract [83]. These reducing agents are able to donate electron pairs to the metals when the reduction occurs on the particles' surface. Also the polyphenols act as capping agent as they introduce negative charge on the reduced metal's surface [83]

After coating of AgNPs with bentonite peaks appeared around 459 cm^{-1}(Si–O–Al), 520 cm^{-1} (Si–O–Mg), (Peaks emerged around 465 cm^{-1} (Si–O–Al), 516 cm^{-1} (Si–O–Mg), and 465 cm^{-1} (Si–O–Mg) when AgNPs were coated with bentonite.). The stretching vibration of Si–O was also attributed to the bands at 1020 and 770 cm^{-1}, which was typically considered as evidence for a three-dimensional amorphous silica phase [135]. The band at 682 cm^{-1} was due to Al–OH, while (Al, Mg)–OH caused the band at 770 cm^{-1}. Si–O–Si bending vibration was attributed to the band between 520 and 459 cm^{-1} [136]. The characteristic AgNPs peak seen at 460 cm^{-1} was symmetric with Si-O-Al. The band observed in the region of 1413-1635 cm^{-1} in both composite reveals that the leaves extract and silver precursor was successfully incorporated with the produced nanoclay. These results confirmed that with the increased amounts of Ag NPs in the Ag-Bent NC at 3438 cm^{-1} broad peak was due to the presence of van der Waals interactions between the hydroxyl groups of MMT layers and the partial positive charge on the surface of Ag-NPs [137].

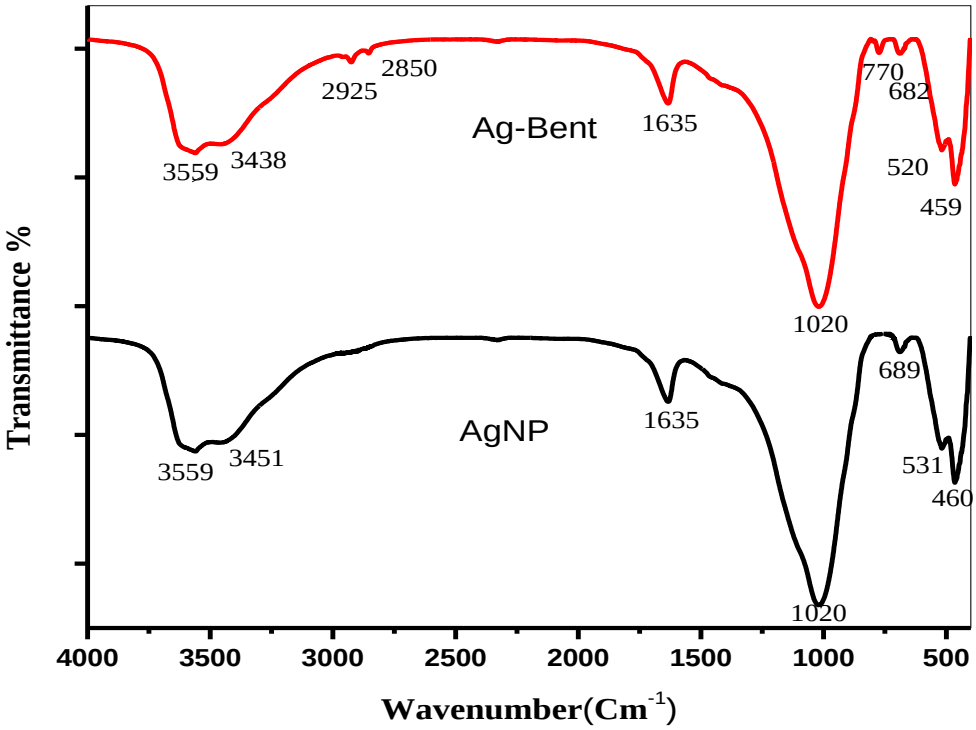

Figure 15: FTIR spectra of Ag NPs and Ag-Bent NCs

4.3.4 Antibacterial Activity Analysis

In this study, *H. abyssinica* plant extract synthesized Ag-Bent NC and Ag NPs at concentration of 125µg/ml, in different ratios and types were tested for antibacterial activity using gram-negative and gram-positive bacteria strains of *Escherichia coli* and *Staphylococcus aureus* using disc diffusion method. Ciprofloxacin was used as positive control.

4.3.4.1 Antibacterial activity of AgNPs

Figure 16 illustrates photographs of the antibacterial tests and the results obtained are summarized and the diameter of inhibition zones (in millimeters) measured is shown in Table 7. The clear zone diameter of the bacterial inhibition zone was correlated to antibiotic activity (ciprofloxacin) for gram-positive and gram-negative bacteria. The presence of an inhibition zone clearly indicates the antibacterial effect of the nanoparticles. Results showed that Ag NPs have significant antimicrobial activity against the tested pathogenic bacteria. The result specify that Ag NPs with the ratio of 1:4 has higher antibacterial activity advantage than Ag NPs with ratio of 1:1 and 1:2. The zone diameter

increased as the size of Ag NPs decreased, because of the bactericidal activity of Ag^{o}. These data are consistent with previously reported studies [133–135]. The zone diameter increased as the size of silver ion-containing Ag nanoparticles decreased, due to bactericide of Ag^{o}. These results may indicate the ability of silver nanoparticles to make silver ions more "antimicrobialy active". All synthesized AgNPs (1:1, 1:2 and 1:4) tested for antibacterial activity showed high activity against *S. aureus* bacteria with inhibition zone of 13nm, 13.5nm and 15nm when compared to *E. coli* bacteria with 11nm, 12nm and 13nm respectively, in comparison to standard antibiotics. It is postulated that the incorporation of silver nanoparticles into the membrane structure occurs. The zone diameter between Ag^{+} ion-containing silver nanoparticles and Ag^{+} ions against *S. aureus* suggest a bacteria membrane exhibiting permeability, leaving the bacterial cells incapable of properly regulating transport through the membrane and causing cell death [141].

The synthesized nanoparticles were smaller than bacteria pore, they could cross the cell membrane freely. Smaller particles having a larger surface area available for interaction will have a stronger bactericidal effect than will larger particle. Ag NPs are able to penetrate the bacteria and cause further damage, possibly by interacting with sulfur- and phosphorus-containing compounds such as DNA [140]. Yuet Yind *et al* reported that the smaller size of AgNPs could cause more toxicity to the bacteria and show better bactericidal effect compared to the larger particles as they have larger surface area [142]. Because of their small particle size, AgNPs can easily reach the nuclear content of bacteria and they show a large and impressive surface area, where contact with bacteria is the greatest [143] and also enable AgNPs to adhere to the cell wall and penetrate into the bacteria cell easily, which in turn improves their antibacterial activity against bacteria [142]. This could be the reason why these nanoparticles have the best antibacterial effect. The presence of AgNPs is very important, which reinforces the idea that the larger the surface area, the greater the antibacterial activity. The diameters of the inhibition zones in agar plates are given in mm below.

The mechanism of action of the antimicrobial activity of silver nanoparticles is based on their penetration in the bacteria cell and reaction with thiol and phosphate groups that are present in membrane proteins or enzymes. Therefore, silver nanoparticles bind to the cell membrane inhibiting cellular respiration and division and leading to cell death.

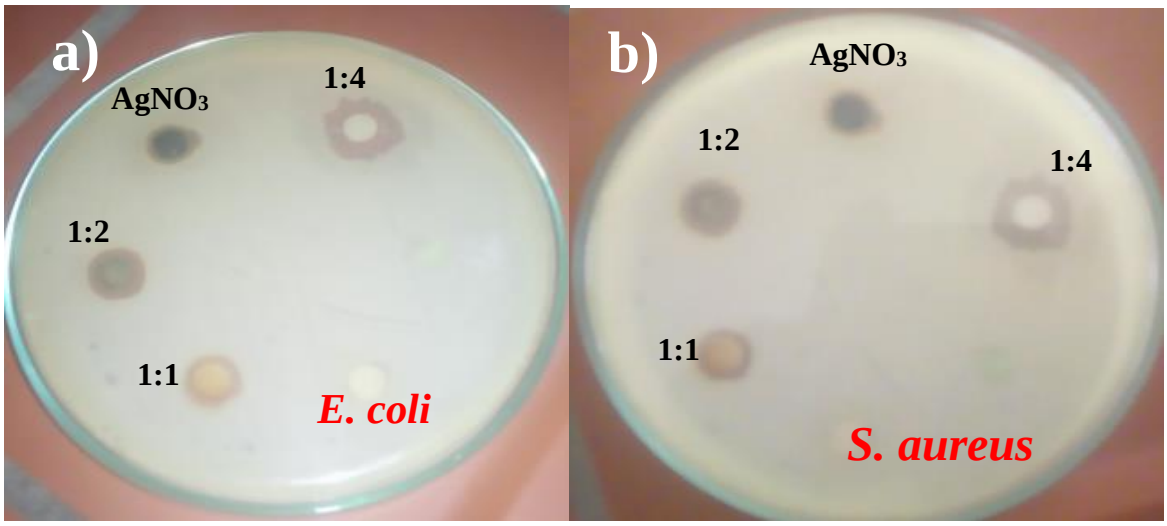

Figure 16: Antibacterial activity of Ag NPs Synthesis by using *H. abyssinica* extract on a) *E.coli* and b) *S. aureus*

Table 7: Antibacterial activity of synthesis Ag NPs

Concentration of Ag NPs (125µg/ml) in different ratios	Zone of inhibition in mm	
	Escherichia coli	*Staphylococcus aureus*
Ag NPs in 1:1	11	13
Ag NPs in 1:2	12	13.5
Ag NPs in 1:4	13	15
$AgNO_3$	7.5	9
Ciprofloxacin	16.5	17

4.3.4.2 Antibacterial activity of Activated-Bent and Ag-Bent

Figure 17 a, b and table 8 antibacterial activity results showed that the Activated- Bent (Na-Bent) has exhibited strong antibacterial activity against both gram-positive *(S. aureus)* and gram-negative *(E. coli)* bacteria than Raw and Ca-Bent (purified). Moreover, Activated-Bent (Na-Bent) performed better antibacterial activity on gram-negative *(E. coli)* bacteria than the gram-positive (*S. aureus*) in comparison to standard antibiotics.

Inhibition zone values were obtained for the synthesized composites of Ag-Bent showed excellent antibacterial property against *E. coli* and *S. aureus* bacteria. The presence of an enhanced inhibition zone clearly unveiled (Figure 17 and table 9) the antibacterial property of the nanocomposites. Table 9 shows that the Ag-Bent (0.2M, 1:4 ratio) had high and remarkable antibacterial activity against gram-negative and gram-positive bacteria better than Ag-Bent (0.1M, 1:2 ratio) and other bentonites because the material contained more silver nanoparticles in its structure. The bactericidal effect of Ag nanoparticles in the composites can be explained by their nano-scale size and exceptional properties. That exhibits pronounced bacterial effects towards a broad range of microorganisms. Their small size (enhanced) allows for better penetration, dispersion and interaction with the bacteria which causes cellular inactivation and disrupting the cell membrane which leads to cell death hence their effectiveness as bactericidal material is increased. Furthermore, a combination of the two composites results an excellent antibacterial activity [144].

Antibacterial activity of the composites can be attributed to chemical and physical properties of the nanoparticles together with the large surface area of the clay. This means that a large amount of nanoparticles with smaller size were highly dispersed per unit area of the bentonite surfaces, thus, maximizing antibacterial activity. In such combinations, nanoparticles are largely attached on bentonite surfaces which ensure uniform dispersion, as unsupported nanoparticles tend to agglomerate and hence reducing their final properties [144]. It has been stated that the release of ions include Ag^{+}, Si^{4+}, Al^{3+}, and Mg^{+} from the nanocomposite are accountable for the exhibited antibacterial property of the materials. Under normal environment, bacterial cell walls are negatively charged due to the presence of carboxyl, hydroxyl, and phosphate groups in lipid bilayer at the cell surface. All released cations from the nanocomposite bind to the above groups that inhibit the normal metabolism of the cellular processes [140,141]. This is the main reason for the antibacterial activity exhibited by the nanocomposites. Ag-Bent nanocomposite is appropriate for a gram-negative *E. coli* bacterium because the outer periplasmic region is very thin and teichoic acid is absent. Because of this reason, nanocomposite material can easily penetrate the cell walls and kill the bacteria [147]. The results also indicated that the examined Ag-Bent nanocomposite was a promising antibacterial material that could kill harmful bacteria.

The different sensitivities of gram positive and gram-negative bacteria could be explained in accordance with the morphological differences between these microorganisms, due to different polarities of their cell membrane. Smaller negative charge *S. aureus* membrane than *E. coli*. This would allow a higher level of penetration of negatively charged free radicals such as, superoxide radical anions and peroxide ions, causing *S. aureus* damage and cell death at lower concentrations than those required to damage *E. coli*.

The prepared *H. abyssinica* mediated AgNPs has the gain of mutual properties of Ag (metal) and *H. abyssinica* (biomaterial). AgNPs have larger surface area. This means that the area for contact with bacteria is higher, which makes AgNPs excellent antibacterial agents.

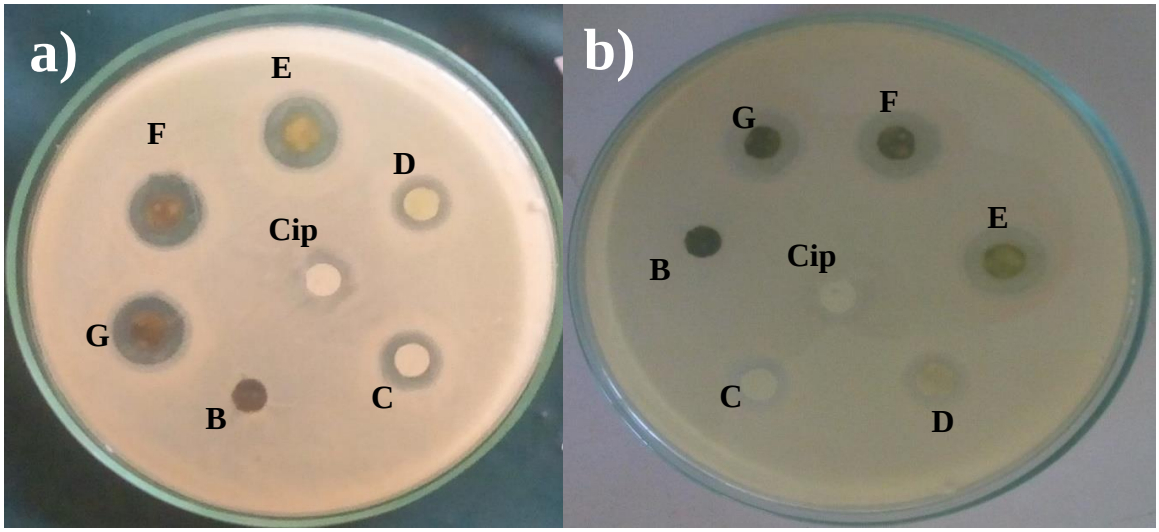

Figure 17: Antibacterial activity of Bent and Ag-Bent NC Synthesis by using *H. abyssinica* extract on a) *E.coli* and b) *S. aureus*

Table 8: Antibacterial activity of Bentonite

Concentration of Bentonite (125µg/ml) in different Types	Zone of inhibition in mm	
	Escherichia coli	*Staphylococcus aureus*
Raw Bentonite(unpurified)- C	13	12
Ca- Bentonite(purified)- D	14	14.5
Na-Activated Bent - G	15	16.5
Ciprofloxacin	16.5	17

Figure 17 table 8 shows the antibacterial activity of activated bentonite. Bentonite was traditionally known clay for healing and treating infections. The antibacterial activity of bentonite clay was found to be very less compared to positive control. The inhibition zone were recorded against *S. aureus* followed by *E.coli*. The inhibition zone is minimum. This might be due to the low concentration of bactericidal mineral present in clay.

The entire bacteria destroyed by the bentonite leachate had significantly higher amounts of Al, P, Fe, Cu, and Pb than the surviving bacteria. Some antibacterial clay's action has been attributed to exchangeable metal ions and the mineralogical makeup of the clay [148].

The activated bentonite treated bacteria had substantially lower Mg and Ca concentrations. This is due to the activation of bentonite with Na^+, which causes ion exchange between Na^+ and Ca^{2+} and Mg^{2+}, resulting in an increase in clay basicity (>10). Because antibacterial clay leachates have a pH of 10, the high concentration of Al in the MMT leachate is also of importance [122].

Table 9: Antibacterial activity of Ag-Bent NCs

Concentration of Ag-Bent NC (125µg/ml) in different ratio	Zone of inhibition in mm	
	Escherichia coli	*Staphylococcus aureus*
Ag-Bent NC(0.1M, 1:2) - F	19	17
Ag-Bent NC(0.2M, 1:4) - E	20	19
Ciprofloxacin	16.5	17

CONCLUSION AND RECOMMENDATION

Conclusion

In this study, AgNP and Ag-Bent have been synthesized successfully via simple and cost-effective Co-precipitation method using *H. abyssinica* leaf that act like both a reducing and capping agent. The Bentonite in the composite were purified and activated. The biosynthesized AgNPs and Ag-Bent NCs were investigated by using different techniques such as X-ray powder Diffractometry (XRD), Fourier transformed Infrared spectroscopy (FTIR) and UV-vis spectroscopy. The crystallinity of AgNPs and Ag-Bent NCs were demonstrated from XRD analysis and the analysis showed all the diffraction peaks fit well with the spherical structure of AgNP and bentonite. The average crystalline size of the AgNPs synthesized from volume ratios of $AgNO_3$ and plant extract were found AgNP(1:1) 23.05nm, AgNPs(1:2) 22.99nm and AgNPs(1:4) 21.76 nm and Average size AgNPs in Ag-Bent NCs synthesized from different concertation of $AgNO_3$ 0.1M (1:2) and 0.2M (1:4) were found to be 10.70nm and 10.34nm respectively. The UV-visible absorption spectra showed the peak characteristic of the SPR band of Ag-NPs (1:4) at 423 nm and 368nm of AgNPs and 488nm of Bentonite in Ag-Bent NCs (0.2M). FT-IR suggested that the interactions between Ag-NPs with the surface of MMT were weak due to the presence of van der Waals interactions. The biosynthesized Ag NPs and Ag-Bent NC were found to have a high antibacterial activity against *S. aureus* and *E. coli*. Generally, addition of silver nanoparticle to the surface of bentonite increase antibacterial activity. The zone of inhibition of AgNPs for 1:4 ratio on gram negative and Ag-Bent for 0.2M 1:4 ratio on gram positive were 15 mm and 20 mm respectively.

Recommendations

Based on the results of this investigation, we recommend;

- ✓ Since the tested compounds displayed potent antibacterial and antioxidant activity, it is necessary to evaluate other activities including antifungal, anticancer, and other activity.
- ✓ In this study, Ag-Bent NPs showed a great antibacterial activity against the bacteria strain, so further studies is suggested to conduct the potential Ag-Bent NCs in the combination with various types of material which is expected to be relevant and advantageous for potential industrial applications.
- ✓ Adsorption parameter such as temperature and pH are important to optimize activity of nanomaterials, but due to time and laboratory facility constraint it was not studied under this research work.
- ✓ It is suggested to take leaching test to evaluate the stability of the nanocomposites.

REFERENCE

[1] S. M. Magaña *et al.*, "Antibacterial activity of montmorillonites modified with silver," *J. Mol. Catal. A Chem.*, vol. 281, no. 1–2, pp. 192–199, 2008.

[2] F. Ohashi, A. Oya, L. Duclaux, and F. Beguin, "Structural model calculation of antimicrobial and antifungal agents derived from clay minerals," *Appl. Clay Sci.*, vol. 12, no. 6, pp. 435–445, 1998.

[3] K. Malachová, P. Praus, Z. Rybková, and O. Kozák, "Antibacterial and antifungal activities of silver, copper and zinc montmorillonites," *Appl. Clay Sci.*, vol. 53, no. 4, pp. 642–645, 2011.

[4] J. Hrenovic, J. Milenkovic, T. Ivankovic, and N. Rajic, "Antibacterial activity of heavy metal-loaded natural zeolite," *J. Hazard. Mater.*, vol. 201–202, pp. 260–264, 2012.

[5] S. Demirci, Z. Ustaoğlu, G. A. Yilmazer, F. Sahin, and N. Baç, "Antimicrobial properties of zeolite-X and zeolite-A ion-exchanged with silver, copper, and zinc against a broad range of microorganisms," *Appl. Biochem. Biotechnol.*, vol. 172, no. 3, pp. 1652–1662, 2014.

[6] M. Isabel Carretero, "Clay minerals and their beneficial effects upon human health. A review," *Appl. Clay Sci.*, vol. 21, pp. 155–163, 2002.

[7] S. C. Motshekga, S. S. Ray, M. S. Onyango, and M. N. B. Momba, "Microwave-assisted synthesis, characterization and antibacterial activity of Ag/ZnO nanoparticles supported bentonite clay," *J. Hazard. Mater.*, vol. 262, pp. 439–446, 2013.

[8] S. Chernousova and M. Epple, "Silver as antibacterial agent: Ion, nanoparticle, and metal," *Angew. Chemie - Int. Ed.*, vol. 52, no. 6, pp. 1636–1653, 2013.

[9] Z. Rahmati, J. Abdi, M. Vossoughi, and I. Alemzadeh, "Ag-doped magnetic metal organic framework as a novel nanostructured material for highly efficient antibacterial activity," *Environ. Res.*, vol. 188, no. April, p. 109555, 2020.

[10] S. Rajakannu, S. Shankar, S. Perumal, and S. Subramanian, "Original Research Article Biosynthesis of Silver Nanoparticles using Garcinia mangostana Fruit

Extract and their Antibacterial , Antioxidant Activity," *Int. J. Curr. Microbiol. Appl. Sci.*, vol. 4, no. 1, pp. 944–952, 2015.

[11] G. Yang, C. Wang, F. Hong, X. Yang, and Z. Cao, "Preparation and characterization of BC/PAM-AgNPs nanocomposites for antibacterial applications," *Carbohydr. Polym.*, vol. 115, pp. 636–642, 2015.

[12] C. Aguzzi *et al.*, "Solid state characterisation of silver sulfadiazine loaded on montmorillonite/chitosan nanocomposite for wound healing," *Colloids Surfaces B Biointerfaces*, vol. 113, pp. 152–157, 2014.

[13] G. F. Cao *et al.*, "Sutures modified by silver-loaded montmorillonite with antibacterial properties," *Appl. Clay Sci.*, vol. 93–94, pp. 102–106, 2014.

[14] A. C. Schneid *et al.*, "Silver nanoparticle-ionic silsesquioxane: A new system proposed as an antibacterial agent," *J. Mater. Chem. B*, vol. 2, no. 8, pp. 1079–1086, 2014.

[15] A. G. R. Targino *et al.*, "An innovative approach to treating dental decay in children. A new anti-caries agent," *J. Mater. Sci. Mater. Med.*, vol. 25, no. 8, pp. 2041–2047, 2014.

[16] J. Slane, J. Vivanco, W. Rose, H. L. Ploeg, and M. Squire, "Mechanical, material, and antimicrobial properties of acrylic bone cement impregnated with silver nanoparticles," *Mater. Sci. Eng. C*, vol. 48, pp. 188–196, 2015.

[17] T. Theivasanthi and M. Alagar, "Anti-bacterial Studies of Silver Nanoparticles," no. 1, 2011.

[18] J. Li, Suyoulema, W. Wang, and Sarina, "A study of photodegradation of sulforhodamine B on Au-TiO2/bentonite under UV and visible light irradiation," *Solid State Sci.*, vol. 11, no. 12, pp. 2037–2043, 2009.

[19] M. Lavorgna *et al.*, "MMT-supported Ag nanoparticles for chitosan nanocomposites: Structural properties and antibacterial activity," *Carbohydr. Polym.*, vol. 102, no. 1, pp. 385–392, 2014.

[20] B. Krishnan and S. Mahalingam, "Improved surface morphology of silver/copper oxide/bentonite nanocomposite using aliphatic ammonium based ionic liquid for enhanced biological activities," *J. Mol. Liq.*, vol. 241, pp. 1044–1058, 2017.

[21] H. Pourabolghasem, M. Ghorbanpour, and R. Shayegh, “Antibacterial activity of copper-doped montmorillonite nanocomposites prepared by alkaline ion exchange method,” *J. Phys. Sci.*, vol. 27, no. 2, pp. 1–12, 2016.

[22] T. Al Ani, “Clay and clay mineralogy,” no. September, 2018.

[23] S. Maisanaba, S. Pichardo, M. Puerto, D. Gutiérrez-Praena, A. M. Cameán, and A. Jos, “Toxicological evaluation of clay minerals and derived nanocomposites: A review,” *Environ. Res.*, vol. 138, pp. 233–254, 2015.

[24] T. Yang, X. D. Wen, J. Li, and L. Yang, “Theoretical and experimental investigations on the structures of purified clay and acid-activated clay,” *Appl. Surf. Sci.*, vol. 252, no. 18, pp. 6154–6161, 2006.

[25] T. Manfredini and M. Hanuskova, “NATURAL RAW MATERIALS IN ‘ TRADITIONAL ’ CERAMIC MANUFACTURING,” pp. 465–470, 2012.

[26] Ö. Şahin, M. Kaya, and C. Saka, “Plasma-surface modification on bentonite clay to improve the performance of adsorption of methylene blue,” *Appl. Clay Sci.*, vol. 116–117, pp. 46–53, 2015.

[27] H. Babaki, A. Salem, and A. Jafarizad, “Kinetic model for the isothermal activation of bentonite by sulfuric acid,” *Mater. Chem. Phys.*, vol. 108, no. 2–3, pp. 263–268, 2008.

[28] W. A. Allo and H. H. Murray, “Mineralogy, chemistry and potential applications of a white bentonite in San Juan province, Argentina,” *Appl. Clay Sci.*, vol. 25, no. 3–4, pp. 237–243, 2004.

[29] M. H. Kim, G. Choi, A. Elzatahry, A. Vinu, Y. Bin Choy, and J. H. Choy, “Review of clay-drug hybrid materials for biomedical applications: Administration routes,” *Clays Clay Miner.*, vol. 64, no. 2, pp. 115–130, 2016.

[30] F. Uddin, “Montmorillonite: An Introduction to Properties and Utilization,” *Curr. Top. Util. Clay Ind. Med. Appl.*, pp. 3–24, 2018.

[31] M. Hayati-Ashtiani and H. Azimi, “Characterization of different types of bentonites and their applications as adsorbents of Co(II) and Ni(II),” *Desalin. Water Treat.*, vol. 57, no. 37, pp. 17384–17399, 2016.

[32] A. M. Fernández, B. Baeyens, M. Bradbury, and P. Rivas, “Analysis of the porewater chemical composition of a Spanish compacted bentonite used in an engineered barrier,” *Phys. Chem. Earth*, vol. 29, no. 1, pp. 105–118, 2004.

[33] G. E. Christidis, A. E. Blum, and D. D. Eberl, “Influence of layer charge and charge distribution of smectites on the flow behaviour and swelling of bentonites,” *Appl. Clay Sci.*, vol. 34, no. 1–4, pp. 125–138, 2006.

[34] D. Doulia, C. Leodopoulos, K. Gimouhopoulos, and F. Rigas, “Adsorption of humic acid on acid-activated Greek bentonite,” *J. Colloid Interface Sci.*, vol. 340, no. 2, pp. 131–141, 2009.

[35] F. Keller-Besrest, S. Benazeth, and C. Souleau, “Pharmaceutical silver doped clays: an EXAFS study from silver to silicon K-edges absorption,” *J. Phys. IV JP*, vol. 4, no. 9, 1994.

[36] M. Zuber, K. M. Zia, S. Mahboob, M. Hassan, and I. A. Bhatti, “Synthesis of chitin-bentonite clay based polyurethane bio-nanocomposites,” *Int. J. Biol. Macromol.*, vol. 47, no. 2, pp. 196–200, 2010.

[37] S. M. Sajadi, K. Kolo, S. M. Hamad, S. A. Mahmud, A. A. Barzinjy, and S. M. Hussein, “Green Synthesis of the Ag/Bentonite Nanocomposite UsingEuphorbia larica Extract: A Reusable Catalyst for Efficient Reduction of Nitro Compounds and Organic Dyes,” *ChemistrySelect*, vol. 3, no. 43, pp. 12274–12280, 2018.

[38] H. Guo *et al.*, “Bioresource Technology Bene fi cial e ff ects of bacterial agent / bentonite on nitrogen transformation and microbial community dynamics during aerobic composting of pig manure,” *Bioresour. Technol.*, vol. 298, no. November 2019, p. 122384, 2020.

[39] A. Rapacz-kmita, M. M. Bu, E. Stodolak-zych, M. Miko, P. Dudek, and M. Trybus, “Characterisation , in vitro release study , and antibacterial activity of montmorillonite-gentamicin complex material,” vol. 70, pp. 471–478, 2017.

[40] C. H. Hu and M. S. Xia, “Adsorption and antibacterial effect of copper-exchanged montmorillonite on Escherichia coli K88,” *Appl. Clay Sci.*, vol. 31, no. 3–4, pp. 180–184, 2006.

[41] N. Meng, N. Zhou, S. Zhang, and J. Shen, “Controlled release and antibacterial

activity chlorhexidine acetate (CA) intercalated in montmorillonite," vol. 382, pp. 45–49, 2009.

[42] S. Park and Y. Jang, "Preparation and characterization of activated carbon fibers supported with silver metal for antibacterial behavior," vol. 261, pp. 238–243, 2003.

[43] I. Sondi and B. Salopek-Sondi, "Silver nanoparticles as antimicrobial agent: A case study on E. coli as a model for Gram-negative bacteria," *J. Colloid Interface Sci.*, vol. 275, no. 1, pp. 177–182, 2004.

[44] J. F. Hernández-Sierra *et al.*, "The antimicrobial sensitivity of Streptococcus mutans to nanoparticles of silver, zinc oxide, and gold," *Nanomedicine Nanotechnology, Biol. Med.*, vol. 4, no. 3, pp. 237–240, 2008.

[45] S. Ahmed, M. Ahmad, B. L. Swami, and S. Ikram, "A review on plants extract mediated synthesis of silver nanoparticles for antimicrobial applications: A green expertise," *J. Adv. Res.*, vol. 7, no. 1, pp. 17–28, 2016.

[46] A. Saxena, R. M. Tripathi, F. Zafar, and P. Singh, "Green synthesis of silver nanoparticles using aqueous solution of Ficus benghalensis leaf extract and characterization of their antibacterial activity," *Mater. Lett.*, vol. 67, no. 1, pp. 91–94, 2012.

[47] V. J. Mohanraj and Y. Chen, "Nanoparticles - A review," *Trop. J. Pharm. Res.*, vol. 5, no. 1, pp. 561–573, 2007.

[48] C. Y. Wu, "Nanoparticles and the environment," *J. Air Waste Manag. Assoc.*, vol. 55, no. 6, pp. 708–746, 2005.

[49] J. H. Thrall, "Nanotechnology and Medicine," *Radiology*, vol. 230, no. 2, pp. 315–318, 2004.

[50] H. Agarwal, S. Venkat Kumar, and S. Rajeshkumar, "A review on green synthesis of zinc oxide nanoparticles – An eco-friendly approach," *Resour. Technol.*, vol. 3, no. 4, pp. 406–413, 2017.

[51] M. A. Gatoo, S. Naseem, M. Y. Arfat, A. Mahmood Dar, K. Qasim, and S. Zubair, "Physicochemical properties of nanomaterials: Implication in associated toxic manifestations," *Biomed Res. Int.*, vol. 2014, 2014.

[52] S. F. Hansen, B. H. Larsen, S. I. Olsen, and A. Baun, “Categorization framework to aid hazard identification of nanomaterials,” *Nanotoxicology*, vol. 1, no. 3, pp. 243–250, 2007.

[53] H. Nadaroglu, A. Alayli, H. Nadaroğlu, A. Alayli Güngör, and S. İnce, “Synthesis of Nanoparticles by Green Synthesis Method,” *Int. J. Innov. Res. Rev.*, vol. 1, no. 1, pp. 6–9, 2017.

[54] I. Khan, K. Saeed, and I. Khan, “Nanoparticles: Properties, applications and toxicities,” *Arab. J. Chem.*, vol. 12, no. 7, pp. 908–931, 2019.

[55] C. P. Devatha and A. K. Thalla, *Green Synthesis of Nanomaterials*. Elsevier Ltd., 2018.

[56] M. A. Huq, “Green synthesis of silver nanoparticles using pseudoduganella eburnea MAHUQ-39 and their antimicrobial mechanisms investigation against drug resistant human pathogens,” *Int. J. Mol. Sci.*, vol. 21, no. 4, 2020.

[57] H. Abdul, R. Sivaraj, and R. Venckatesh, “Green synthesis and characterization of zinc oxide nanoparticles from Ocimum basilicum L . var . purpurascens Benth . - Lamiaceae leaf extract,” *Mater. Lett.*, vol. 131, pp. 16–18, 2014.

[58] M. Heinlaan, A. Ivask, I. Blinova, H. Dubourguier, and A. Kahru, “Toxicity of nanosized and bulk ZnO , CuO and TiO 2 to bacteria Vibrio fischeri and crustaceans Daphnia magna and Thamnocephalus platyurus,” vol. 71, pp. 1308–1316, 2008.

[59] J. Qu, X. Yuan, X. Wang, and P. Shao, “Zinc accumulation and synthesis of ZnO nanoparticles using Physalis alkekengi L .,” *Environ. Pollut.*, vol. 159, no. 7, pp. 1783–1788, 2011.

[60] C. R. Galan, M. F. Silva, D. Mantovani, R. Bergamasco, and M. F. Vieira, “Green synthesis of copper oxide nanoparticles impregnated on activated carbon using Moringa oleifera leaves extract for the removal of nitrates from water,” *Can. J. Chem. Eng.*, vol. 96, no. 11, pp. 2378–2386, 2018.

[61] S. V Otari, R. M. Patil, S. J. Ghosh, and S. H. Pawar, “Green phytosynthesis of silver nanoparticles using aqueous extract of Manilkara zapota (L .) seeds and its inhibitory action against Candida species,” *Mater. Lett.*, vol. 116, pp. 367–369, 2014.

[62] M. Ghaedi, M. Yousefinejad, M. Safarpoor, H. Z. Khafri, and M. K. Purkait, "Journal of Industrial and Engineering Chemistry Rosmarinus officinalis leaf extract mediated green synthesis of silver nanoparticles and investigation of its antimicrobial properties," *J. Ind. Eng. Chem.*, vol. 31, pp. 167–172, 2015.

[63] S. Hemmati, A. Rashtiani, M. Mahdi, and P. Mohammadi, "Green synthesis and characterization of silver nanoparticles using Fritillaria flower extract and their antibacterial activity against some human pathogens," *Polyhedron*, vol. 158, no. May 2014, pp. 8–14, 2019.

[64] M. Hekmati, S. Hasanirad, A. Khaledi, and D. Esmaeili, "Gene Reports Green synthesis of silver nanoparticles using extracts of Allium rotundum l , Falcaria vulgaris Bernh , and Ferulago angulate Boiss , and their antimicrobial e ff ects in vitro," *Gene Reports*, vol. 19, no. December 2019, p. 100589, 2020.

[65] M. Ali, B. Kim, K. D. Bel, D. Norman, M. Brennan, and G. Shad, "Green synthesis and characterization of silver nanoparticles using Artemisia absinthium aqueous extract — A comprehensive study," vol. 58, pp. 359–365, 2016.

[66] H. Bar, D. K. Bhui, G. P. Sahoo, P. Sarkar, S. P. De, and A. Misra, "Colloids and Surfaces A : Physicochemical and Engineering Aspects Green synthesis of silver nanoparticles using latex of Jatropha curcas," vol. 339, pp. 134–139, 2009.

[67] S. Li *et al.*, "Green synthesis of silver nanoparticles using Capsicum annuum L . extract {," pp. 852–858, 2007.

[68] A. M. Awwad and N. M. Salem, "Green Synthesis of Silver Nanoparticles byMulberry LeavesExtract," no. October, pp. 1–5, 2012.

[69] M. S. Aref and S. S. Salem, "Biocatalysis and Agricultural Biotechnology Bio - callus synthesis of silver nanoparticles , characterization , and antibacterial activities via Cinnamomum camphora callus culture," *Biocatal. Agric. Biotechnol.*, vol. 27, no. March, p. 101689, 2020.

[70] N. Krithiga, A. Rajalakshmi, and A. Jayachitra, "Green Synthesis of Silver Nanoparticles Using Leaf Extracts of Clitoria ternatea and Solanum nigrum and Study of Its Antibacterial Effect against Common Nosocomial Pathogens," *J. Nanosci.*, vol. 2015, pp. 1–8, 2015.

[71] M. Ghaffari-moghaddam and R. Hadi-dabanlou, “Journal of Industrial and Engineering Chemistry Plant mediated green synthesis and antibacterial activity of silver nanoparticles using Crataegus douglasii fruit extract,” *J. Ind. Eng. Chem.*, vol. 20, no. 2, pp. 739–744, 2014.

[72] A. Angel Ezhilarasi, J. Judith Vijaya, K. Kaviyarasu, L. John Kennedy, R. J. Ramalingam, and H. A. Al-Lohedan, “Rapid biosynthesis and characterization of silver nanoparticles from the leaf extract of Tropaeolum majus L. and its enhanced in-vitro antibacterial, antifungal, antioxidant and anticancer properties,” *J. Photochem. Photobiol. B Biol.*, vol. 180, pp. 39–50, 2019.

[73] E. Filippo, A. Serra, A. Buccolieri, and D. Manno, “Green synthesis of silver nanoparticles with sucrose and maltose : Morphological and structural characterization,” *J. Non. Cryst. Solids*, vol. 356, no. 6–8, pp. 344–350, 2010.

[74] T. Wolde, B. Bizuayehu, T. Hailemariam, and K. Tiruha, “ Phytochemical analysis and Antimicrobial activity of Hagenia Abyssinica ,” *Indian J. Pharm. Pharmacol.*, vol. 3, no. 3, p. 127, 2016.

[75] Z. D. Kifle, B. B. Kidanu, T. Y. Tadesse, T. F. Belachew, and S. A. Atnafie, “Evaluation of in Vivo Antidiarrheal Activity of Solvent Fractions of Hagenia abyssinica (Rosaceae) in Swiss Albino Mice,” *Evidence-based Complement. Altern. Med.*, vol. 2021, 2021.

[76] T. Feyissa, M. Welander, and L. Negash, “Micropropagation of Hagenia abyssinica: A multipurpose tree,” *Plant Cell. Tissue Organ Cult.*, vol. 80, no. 2, pp. 119–127, 2005.

[77] L. Negash, *Indigenous trees of Ethiopia: biology, uses and propagation techniques*, no. March. 1995.

[78] T. Feyissa, H. Nybom, I. V. Bartish, and M. Welander, “Analysis of genetic diversity in the endangered tropical tree species Hagenia abyssinica using ISSR markers,” *Genet. Resour. Crop Evol.*, vol. 54, no. 5, pp. 947–958, 2007.

[79] K. W. Index-cdisfemon, “Phloroglucinol derivatives of,” vol. 4, no. I, pp. 7–8, 1977.

[80] B. Assefa, G. Glatzel, and C. Buchmann, “Ethnomedicinal uses of Hagenia

abyssinica (Bruce) J.F. Gmel. among rural communities of Ethiopia," *J. Ethnobiol. Ethnomed.*, vol. 6, pp. 1–10, 2010.

[81] H. C. A. Murthy, T. Desalegn, M. Kassa, B. Abebe, and T. Assefa, "Synthesis of Green Copper Nanoparticles Using Medicinal Plant Hagenia abyssinica (Brace) JF. Gmel. Leaf Extract: Antimicrobial Properties," *J. Nanomater.*, vol. 2020, 2020.

[82] H. C. Ananda Murthy, T. Desalegn Zeleke, C. R. Ravikumar, M. R. Anil Kumar, and H. P. Nagaswarupa, "Electrochemical properties of biogenic silver nanoparticles synthesized using Hagenia abyssinica (Brace) JF. Gmel. medicinal plant leaf extract," *Mater. Res. Express*, vol. 7, no. 5, 2020.

[83] W. W. Melkamu and L. T. Bitew, "Green synthesis of silver nanoparticles using Hagenia abyssinica (Bruce) J.F. Gmel plant leaf extract and their antibacterial and anti-oxidant activities," *Heliyon*, vol. 7, no. 11, p. e08459, 2021.

[84] M. Kilonzo and D. Munisi, "Antimicrobial activities and phytochemical analysis of Harrisonia abyssinica (Oliv) and Vepris simplicifolia (Verd) extracts used as traditional medicine in Tanzania," *Saudi J. Biol. Sci.*, vol. 28, no. 12, pp. 7481–7485, 2021.

[85] S. B. Obakiro *et al.*, "Traditional Medicinal Uses, Phytoconstituents, Bioactivities, and Toxicities of Erythrina abyssinica Lam. ex DC. (Fabaceae): A Systematic Review," *Evidence-based Complement. Altern. Med.*, vol. 2021, 2021.

[86] S. Komarneni, "Nanocornposites," vol. 2, no. 12, pp. 1219–1230, 1992.

[87] S. Kumar, C. Guria, and A. Mandal, "Synthesis, characterization and performance studies of polysulfone/bentonite nanoparticles mixed-matrix ultra-filtration membranes using oil field produced water," *Sep. Purif. Technol.*, vol. 150, pp. 145–158, 2015.

[88] V. Bahadur, R. Gadi, and S. Kalra, "Clay based nanocomposites for removal of heavy metals from water : A review," *J. Environ. Manage.*, vol. 232, no. December 2018, pp. 803–817, 2019.

[89] T. Guo, S. Cao, R. Su, Z. Li, P. Hu, and Z. Xu, "Adsorptive property of Cu 2+-loaded montmorillonite clays for Escherichia coli K 88 in vitro," *J. Environ. Sci.*, vol. 23, no. 11, pp. 1808–1815, 2011.

[90] B. Bagchi *et al.*, “In situ synthesis and antibacterial activity of copper nanoparticle loaded natural montmorillonite clay based on contact inhibition and ion release,” *Colloids Surfaces B Biointerfaces*, vol. 108, pp. 358–365, 2013.

[91] Y. Zhou, M. Xia, Y. Ye, and C. Hu, “Antimicrobial ability of Cu2+-montmorillonite,” *Appl. Clay Sci.*, vol. 27, no. 3–4, pp. 215–218, 2004.

[92] H. He, D. Yang, P. Yuan, W. Shen, and R. L. Frost, “A novel organoclay with antibacterial activity prepared from montmorillonite and Chlorhexidini Acetas,” *J. Colloid Interface Sci.*, vol. 297, no. 1, pp. 235–243, 2006.

[93] H. Pouraboulghasem, M. Ghorbanpour, R. Shayegh, and S. Lotfiman, “Synthesis, characterization and antimicrobial activity of alkaline ion-exchanged ZnO/bentonite nanocomposites,” *J. Cent. South Univ.*, vol. 23, no. 4, pp. 787–792, 2016.

[94] C. H. Hu, Z. R. Xu, and M. S. Xia, “Antibacterial effect of Cu2+-exchanged montmorillonite on Aeromonas hydrophila and discussion on its mechanism,” *Vet. Microbiol.*, vol. 109, no. 1–2, pp. 83–88, 2005.

[95] S. Shrivastava, T. Bera, A. Roy, G. Singh, P. Ramachandrarao, and D. Dash, “Characterization of enhanced antibacterial effects of novel silver nanoparticles,” *Nanotechnology*, vol. 18, no. 22, 2007.

[96] S. Hamed, M. Emara, R. M. Shawky, R. A. El-domany, and T. Youssef, “Silver nanoparticles: Antimicrobial activity, cytotoxicity, and synergism with N-acetyl cysteine,” *J. Basic Microbiol.*, vol. 57, no. 8, pp. 659–668, 2017.

[97] H. L. Su *et al.*, “The disruption of bacterial membrane integrity through ROS generation induced by nanohybrids of silver and clay,” *Biomaterials*, vol. 30, no. 30, pp. 5979–5987, 2009.

[98] H. Wang and P. K. Chu, *Surface Characterization of Biomaterials*. Elsevier, 2013.

[99] H. Senoussi, H. Osmani, C. Courtois, and M. E. H. Bourahli, “Mineralogical and chemical characterization of DD3 kaolin from the east of Algeria,” *Bol. la Soc. Esp. Ceram. y Vidr.*, vol. 55, no. 3, pp. 121–126, 2016.

[100] R. McCuen, “Book Reviews: Book Reviews,” *JAWRA J. Am. Water Resour. Assoc.*, vol. 48, no. 5, pp. 1071–1073, 2012.

[101] D. D. Eberl, Ś. Jan, H. R. Northrop, and E. E. T. Al, “Potassium F i x a t i o n i n Smectite by Wetting a n d D r y i n g U . S . Geological Survey , Box 25046 , Federal Center , Mail Stop 404 , Denver , CO 8 Institute of Geological Sciences , Polish Academy of Sciences , 31-002 Krakow , Senacka 3 , Poland P,” 1986.

[102] S. Muthukumaran and R. Gopalakrishnan, “Structural, FTIR and photoluminescence studies of Cu doped ZnO nanopowders by co-precipitation method,” *Opt. Mater. (Amst).*, vol. 34, no. 11, pp. 1946–1953, 2012.

[103] J. W. Robinson, “Atomic Absorption Spectroscopy,” *Anal. Chem.*, vol. 32, no. 8, pp. 17A-29A, 1960.

[104] S. Y. C. Tong, J. S. Davis, E. Eichenberger, T. L. Holland, and V. G. Fowler, “Staphylococcus aureus infections: Epidemiology, pathophysiology, clinical manifestations, and management,” *Clin. Microbiol. Rev.*, vol. 28, no. 3, pp. 603–661, 2015.

[105] D. D. Bannerman, M. J. Paape, J. W. Lee, X. Zhao, J. C. Hope, and P. Rainard, “Escherichia coli and Staphylococcus aureus elicit differential innate immune responses following intramammary infection,” *Clin. Diagn. Lab. Immunol.*, vol. 11, no. 3, pp. 463–472, 2004.

[106] S. Ahmed, Saifullah, M. Ahmad, B. L. Swami, and S. Ikram, “ Green synthesis of silver nanoparticles using Azadirachta indica aqueous leaf extract ,” *J. Radiat. Res. Appl. Sci.*, vol. 9, no. 1, pp. 1–7, 2016.

[107] H. O. Edeoga, D. E. Okwu, and B. O. Mbaebie, “Phytochemical constituents of some Nigerian medicinal plants,” *African J. Biotechnol.*, vol. 4, no. 7, pp. 685–688, 2005.

[108] M. S. Auwal, S. Saka, I. A. Mairiga, K. A. Sanda, A. Shuaibu, and A. Ibrahim, “Preliminary phytochemical and elemental analysis of aqueous and fractionated pod extracts of Acacia nilotica (Thorn mimosa).,” *Vet. Res. forum an Int. Q. J.*, vol. 5, no. 2, pp. 95–100, 2014.

[109] R. Tanaka, S. Matsunanga, and T. Sasaki, “A new flavanone derivative from the leaves of Tsuga diversifolia,” *Planta Med.*, vol. 55, no. 6, pp. 570–571, 1989.

[110] N. Yildiz, Y. Sarikaya, and A. Çalimli, “The effect of the electrolyte concentration

and pH on the rheological properties of the original and the Na2CO3-activated Kutahya bentonite," *Appl. Clay Sci.*, vol. 14, no. 5–6, pp. 319–327, 1999.

[111] L. A. Shah, N. S. Khattak, M. G. S. Valenzuela, A. Manan, and F. R. Valenzuela Díaz, "Preparation and characterization of purified Na-activated bentonite from Karak (Pakistan) for pharmaceutical use," *Clay Miner.*, vol. 48, no. 4, pp. 595–603, 2013.

[112] K. Shameli, M. Bin Ahmad, M. Zargar, W. M. Z. W. Yunus, A. Rustaiyan, and N. A. Ibrahim, "Synthesis of silver nanoparticles in montmorillonite and their antibacterial behavior.," *Int. J. Nanomedicine*, vol. 6, pp. 581–590, 2011.

[113] M. B. Bazbouz, *Preparation of Sodium-Activated Natural Bentonite Clay Incorporated Cellulose Acetate Nanofibres by Free Surface Electrospinning and Its Proposed Applications*. 2018.

[114] T. Fatima, S. Rafiq, A. Iqbal, and S. Husnain, "Prevalence and Antibiogram of MDR E. coli Strains Isolated from UTI Patients—1-Year Retrospective Study at Nishtar Medical Hospital, Multan," *SN Compr. Clin. Med.*, vol. 2, no. 4, pp. 423–431, 2020.

[115] P. Murugesan, "Phytochemical Analysis and Antimicrobial Activity of Edible Lichen," *J. Drug Deliv. Ther.*, vol. 10, no. 2-s, pp. 102–104, 2020.

[116] R. R. Unnithan, "Characterization of Na 2 CO 3 activated Calcium Bentonite and its application as a GCL," vol. 5, no. 08, pp. 3–6, 2017.

[117] H. Bar, D. K. Bhui, G. P. Sahoo, P. Sarkar, S. Pyne, and A. Misra, "Green synthesis of silver nanoparticles using seed extract of Jatropha curcas," *Colloids Surfaces A Physicochem. Eng. Asp.*, vol. 348, no. 1–3, pp. 212–216, 2009.

[118] S. Bykkam, M. Ahmadipour, S. Narisngam, V. R. Kalagadda, and S. C. Chidurala, "RETRACTED: Extensive Studies on X-Ray Diffraction of Green Synthesized Silver Nanoparticles," *Adv. Nanoparticles*, vol. 04, no. 01, pp. 1–10, 2015.

[119] I. A. Wani, A. Ganguly, J. Ahmed, and T. Ahmad, "Silver nanoparticles: Ultrasonic wave assisted synthesis, optical characterization and surface area studies," *Mater. Lett.*, vol. 65, no. 3, pp. 520–522, 2011.

[120] R. Sathyavathi, M. B. M. Krishna, and D. N. Rao, "Biosynthesis of Silver

Nanoparticles Using Moringa oleifera Leaf Extract and Its Application to Optical Limiting," vol. 11, no. 3, pp. 2031–2035, 2011.

[121] H. P. Borase *et al.*, "Plant extract: A promising biomatrix for ecofriendly, controlled synthesis of silver nanoparticles," *Appl. Biochem. Biotechnol.*, vol. 173, no. 1, pp. 1–29, 2014.

[122] M. Naswir, S. Arita, Marsi, and Salni, "Characterization of Bentonite by XRD and SEM-EDS and Use to Increase PH and Color Removal, Fe and Organic Substances in Peat Water," *J. Clean Energy Technol.*, vol. 1, no. 4, pp. 313–317, 2013.

[123] F. Azarbani and S. Shiravand, "Green synthesis of silver nanoparticles by Ferulago macrocarpa flowers extract and their antibacterial, antifungal and toxic effects," *Green Chem. Lett. Rev.*, vol. 13, no. 1, pp. 41–49, 2020.

[124] A. R. Deshmukh, A. Gupta, and B. S. Kim, "Ultrasound Assisted Green Synthesis of Silver and Iron Oxide Nanoparticles Using Fenugreek Seed Extract and Their Enhanced Antibacterial and Antioxidant Activities," *Biomed Res. Int.*, vol. 2019, 2019.

[125] V. Amendola, O. M. Bakr, and F. Stellacci, "A study of the surface plasmon resonance of silver nanoparticles by the discrete dipole approximation method: Effect of shape, size, structure, and assembly," *Plasmonics*, vol. 5, no. 1, pp. 85–97, 2010.

[126] B. Chudasama, A. K. Vala, N. Andhariya, R. V Upadhyay, and R. V Mehta, "Antifungal activity of multifunctional Fe3O4Ag nanocolloids," in *Journal of Magnetism and Magnetic Materials*, 2011, vol. 323, no. 10, pp. 1233–1237.

[127] A. Mishra, A. Mehta, M. Sharma, and S. Basu, "Impact of Ag nanoparticles on photomineralization of chlorobenzene by TiO2/bentonite nanocomposite," *J. Environ. Chem. Eng.*, vol. 5, no. 1, pp. 644–651, 2017.

[128] O. A. Yeshchenko, I. M. Dmitruk, A. A. Alexeenko, A. V. Kotko, J. Verdal, and A. O. Pinchuk, "Size and Temperature Effects on the Surface Plasmon Resonance in Silver Nanoparticles," *Plasmonics*, vol. 7, no. 4, pp. 685–694, 2012.

[129] S. C. Motshekga, S. S. Ray, M. S. Onyango, and M. N. B. Momba, "Preparation and antibacterial activity of chitosan-based nanocomposites containing bentonite-

supported silver and zinc oxide nanoparticles for water disinfection," *Appl. Clay Sci.*, vol. 114, pp. 330–339, 2015.

[130] M. Sirait, N. Bukit, and N. Siregar, "Preparation and characterization of natural bentonite in to nanoparticles by co-precipitation method," *AIP Conf. Proc.*, vol. 1801, no. January, 2017.

[131] K. Fisseha, "Modification of Bentonite Clay for Adsorption Enhancement for Congo Red Dye Removal from Textile Waste Water Modification of Bentonite Clay for Adsorption Enhancement for Congo red Dye Removal from Textile Waste Water," 2017.

[132] Z. Movasaghi, S. Rehman, and I. U. Rehman, "Fourier transform infrared (FTIR) spectroscopy of biological tissues," *Appl. Spectrosc. Rev.*, vol. 43, no. 2, pp. 134–179, 2008.

[133] G. Maheshwaran, M. Malai Selvi, R. Selva Muneeswari, A. Nivedhitha Bharathi, M. Krishna Kumar, and S. Sudhahar, "Green synthesis of lanthanum oxide nanoparticles using Moringa oleifera leaves extract and its biological activities," *Adv. Powder Technol.*, vol. 32, no. 6, pp. 1963–1971, 2021.

[134] K. Shameli *et al.*, "Green biosynthesis of silver nanoparticles using callicarpa maingayi stem bark extraction," *Molecules*, vol. 17, no. 7, pp. 8506–8517, 2012.

[135] H. Yang, C. Du, S. Jin, and A. Tang, "Preparation and characterization of SnO2 nanoparticles incorporated into talc porous materials (TPM)," *Mater. Lett.*, vol. 61, no. 17, pp. 3736–3739, 2007.

[136] A. Alemdar, N. Güngör, O. I. Ece, and O. Atici, "The rheological properties and characterization of bentonite dispersions in the presence of non-ionic polymer PEG," *J. Mater. Sci.*, vol. 40, no. 1, pp. 171–177, 2005.

[137] Z. Yang, H. Peng, W. Wang, and T. Liu, "Crystallization behavior of poly(ε-caprolactone)/layered double hydroxide nanocomposites," *J. Appl. Polym. Sci.*, vol. 116, no. 5, pp. 2658–2667, 2010.

[138] A. Al-Sharqi, K. Apun, M. Vincent, D. Kanakaraju, and L. M. Bilung, "Enhancement of the antibacterial efficiency of silver nanoparticles against gram-positive and gram-negative bacteria using blue laser light," *Int. J. Photoenergy*, vol.

2019, 2019.

[139] T. Bruna, F. Maldonado-Bravo, P. Jara, and N. Caro, “Silver nanoparticles and their antibacterial applications,” *Int. J. Mol. Sci.*, vol. 22, no. 13, 2021.

[140] M. Guzman, J. Dille, and S. Godet, “Synthesis and antibacterial activity of silver nanoparticles against gram-positive and gram-negative bacteria,” *Nanomedicine Nanotechnology, Biol. Med.*, vol. 8, no. 1, pp. 37–45, 2012.

[141] J. S. Kim, “Antibacterial activity of Ag+ion-containing silver nanoparticles prepared using the alcohol reduction method,” *J. Ind. Eng. Chem.*, vol. 13, no. 5, pp. 718–722, 2007.

[142] Y. Y. Loo *et al.*, “In Vitro antimicrobial activity of green synthesized silver nanoparticles against selected Gram-negative foodborne pathogens,” *Front. Microbiol.*, vol. 9, no. JUL, pp. 1–7, 2018.

[143] K. Shameli *et al.*, “Synthesis and characterization of silver/montmorillonite/chitosan bionanocomposites by chemical reduction method and their antibacterial activity.,” *Int. J. Nanomedicine*, vol. 6, pp. 271–284, 2011.

[144] S. C. Motshekga, S. S. Ray, M. S. Onyango, and M. N. B. Momba, “Microwave-assisted synthesis, characterization and antibacterial activity of Ag/ZnO nanoparticles supported bentonite clay,” *J. Hazard. Mater.*, vol. 262, pp. 439–446, 2013.

[145] A. Azam, A. S. Ahmed, M. Oves, M. S. Khan, and A. Memic, “Size-dependent antimicrobial properties of CuO nanoparticles against Gram-positive and -negative bacterial strains,” *Int. J. Nanomedicine*, vol. 7, pp. 3527–3535, 2012.

[146] S. H. Sohrabnezhad, M. J. Mehdipour Moghaddam, and T. Salavatiyan, “Synthesis and characterization of CuO-montmorillonite nanocomposite by thermal decomposition method and antibacterial activity of nanocomposite,” *Spectrochim. Acta - Part A Mol. Biomol. Spectrosc.*, vol. 125, pp. 73–78, 2014.

[147] B. Krishnan and S. Mahalingam, “Ag/TiO2/bentonite nanocomposite for biological applications: Synthesis, characterization, antibacterial and cytotoxic investigations,” *Adv. Powder Technol.*, vol. 28, no. 9, pp. 2265–2280, 2017.

[148] S. E. Haydel, C. M. Remenih, and L. B. Williams, “Broad-spectrum in vitro

antibacterial activities of clay minerals against antibiotic-susceptible and antibiotic-resistant bacterial pathogens," *J. Antimicrob. Chemother.*, vol. 61, no. 2, pp. 353–361, 2008.